SUPPLEMENTARY MATERIALS FOR "ESTIMATING GLOBAL AND COUNTRY-SPECIFIC EXCESS MORTALITY DURING THE COVID-19 PANDEMIC"

BY VICTORIA KNUTSON[1], SERGE ALESHIN-GUENDEL[1], ARIEL KARLINSKY[2], WILLIAM MSEMBURI[3], JON WAKEFIELD[1,4],

[1]*Department of Biostatistics, University of Washington, Seattle, USA*

[2]*Hebrew University, Jerusalem, Israel*

[3]*World Health Organisation, Geneva, Switzerland*

[4]*Department of Statistics, University of Washington, Seattle, USA*

1. Modeling Framework. In this section we discuss the overview of the modeling framework. The excess is defined as the observed all-cause mortality (ACM) minus the expected ACM. Modeling is required to obtain the latter. If ACM data were available for all countries during historic and pandemic then we would only need to model the historic data to produce expected numbers (assuming that there were no issues of undercount or late registration).

One approach, for countries have full ACM data, would be to model the historic and pandemic data simultaneously. For example, one could include in a model seasonable terms and a long-term trend, and then have an indicator for pandemic times. However, the aim of our modeling of pandemic data (for those countries that have it), is to construct a predictive model for those countries who have not provided ACM data in the pandemic, using country-specific covariates. Many of these covariates vary by month, and we wish the "signal" during the pandemic to be attributed to the covariates, rather than country-specific seasonality terms. Hence, we first model the historic period data (to create expected numbers), and then, conditional on the expected numbers, model the pandemic data. The expected numbers modeling is done for all countries, regardless of the data they have available in the pandemic. Recall, the excess

$$\delta_{c,t} = y_{c,t} - E_{c,t},$$

and the first term on the RHS is known for countries with full data, in which case the posterior for $\delta_{c,t}$ is based on the posterior for $E_{c,t}$ only.

	Full Data	Subnational Data	Annual Data	No Data	All Data
Historic	$\boldsymbol{y}^{\text{hf}}$	$\boldsymbol{y}^{\text{hs}}$	$\boldsymbol{y}^{\text{ha}}$	$\boldsymbol{y}^{\text{hn}}$	$\boldsymbol{y}^{\text{h}}$
Pandemic	$\boldsymbol{y}^{\text{pf}}$	$\boldsymbol{y}^{\text{ps}}$	$\boldsymbol{y}^{\text{pa}}$	$\boldsymbol{y}^{\text{pn}}$	$\boldsymbol{y}^{\text{p}}$
Expected	$\boldsymbol{E}^{\text{f}}$	$\boldsymbol{E}^{\text{s}}$	$\boldsymbol{E}^{\text{a}}$	$\boldsymbol{E}^{\text{n}}$	$\boldsymbol{E}$
Covariates	$\boldsymbol{x}^{\text{f}}$	Not used	$\boldsymbol{x}^{\text{a}}$	$\boldsymbol{x}^{\text{n}}$	$\boldsymbol{x}$

TABLE 1

Notation by data types in historic and pandemic times; $\boldsymbol{y}^{pn}$ is unobserved.

Table 1 summarizes the notation for the data we have available. We let $\boldsymbol{\phi}$ represent the parameters of the models that are used to calculate the expected numbers and $\boldsymbol{\lambda}$ the parameters that are used to model the pandemic data. The posterior for the unknown parameters is:

$$\begin{aligned}\pi(\boldsymbol{\phi}, \boldsymbol{\lambda} | \boldsymbol{y}^{\text{h}}, \boldsymbol{y}^{\text{p}}, \boldsymbol{E}, \boldsymbol{x}) &\propto p(\boldsymbol{y}^{\text{h}}, \boldsymbol{y}^{\text{p}} | \boldsymbol{\phi}, \boldsymbol{\lambda}, \boldsymbol{E}, \boldsymbol{x}) \times \pi(\boldsymbol{\phi}, \boldsymbol{\lambda}) \\ &= p(\boldsymbol{y}^{\text{h}} | \boldsymbol{\phi}) \pi(\boldsymbol{\phi}) \times p(\boldsymbol{y}^{\text{p}} | \boldsymbol{\lambda}, \boldsymbol{E}, \boldsymbol{x}) \pi(\boldsymbol{\lambda})\end{aligned}$$

where $\boldsymbol{E} = \boldsymbol{E}(\phi, \boldsymbol{y}^{\mathrm{h}})$. We next discuss the modeling of each of the historic and pandemic data.

The posterior for the parameters ϕ in the expected numbers model is:

$$p(\phi|\boldsymbol{y}^{\mathrm{h}}) \propto \underbrace{p(\boldsymbol{y}^{\mathrm{h}}|\phi)}_{\text{Expecteds Model}} \times \pi(\phi).$$

This posterior is approximated using the `mgcv` library `gam` function (Wood, 2017, Section 6.10).

We let $\boldsymbol{\lambda} = (\boldsymbol{\theta}, \boldsymbol{p})$ where $\boldsymbol{\theta}$ are the parameters of the covariate model and $\boldsymbol{p}$ the parameters of the subnational multinomial model. For the annual data we use a mulitnomial model with the probabilities depending on the covariate model. The posterior is,

$$\begin{aligned}
\pi(\boldsymbol{\theta}, \boldsymbol{p}|\boldsymbol{y}^{\mathrm{pf}}, \boldsymbol{y}^{\mathrm{ps}}, \boldsymbol{y}^{\mathrm{pa}}, \boldsymbol{E}^{\mathrm{f}}, \boldsymbol{E}^{\mathrm{a}}, \boldsymbol{x}^{\mathrm{f}}, \boldsymbol{x}^{\mathrm{a}}) &\propto p(\boldsymbol{y}^{\mathrm{pf}}, \boldsymbol{y}^{\mathrm{ps}}, \boldsymbol{y}^{\mathrm{pa}}|\boldsymbol{\theta}, \boldsymbol{p}, \boldsymbol{E}^{\mathrm{f}}, \boldsymbol{E}^{\mathrm{a}}, \boldsymbol{x}^{\mathrm{f}}, \boldsymbol{x}^{\mathrm{a}}) \times \pi(\boldsymbol{\theta}, \boldsymbol{p}) \\
&= \underbrace{p(\boldsymbol{y}^{\mathrm{pf}}|\boldsymbol{\theta}, \boldsymbol{E}^{\mathrm{f}}, \boldsymbol{x}^{\mathrm{f}}) \times \pi(\boldsymbol{\theta})}_{\text{Covariate Model}} \\
&\times \underbrace{p(\boldsymbol{y}^{\mathrm{ps}}|\boldsymbol{p}) \times \pi(\boldsymbol{p})}_{\text{Subnational Model}} \\
&\times \underbrace{p(\boldsymbol{y}^{\mathrm{pa}}|\boldsymbol{\theta}, \boldsymbol{E}^{\mathrm{a}}, \boldsymbol{x}^{\mathrm{a}})}_{\text{Annual Model}}.
\end{aligned}$$

We can factor the above into two pieces: the $\boldsymbol{\theta}$ parameters from the covariate model and annual models, and the $\boldsymbol{p}$ parameters from the subnational model. Note that there are very few annual data countries and for practical reasons we estimate the $\boldsymbol{\theta}$ parameters from the covariate model, and then used samples from the posterior to estimate the monthly contributions to the annual data. Predictive distributions are constructed for the total ACM counts for the no data countries, using

$$p(\boldsymbol{y}^{\mathrm{pn}}|\boldsymbol{\theta}, \boldsymbol{x}^{\mathrm{n}}),$$

which is a negative binomial distribution.

To obtain the posterior for the excess $\boldsymbol{\delta}^{\mathrm{f}}, \boldsymbol{\delta}^{\mathrm{s}}, \boldsymbol{\delta}^{\mathrm{a}}, \boldsymbol{\delta}^{\mathrm{n}}$ for countries with full, subnational, annual and no data, respectively, note that $\boldsymbol{\delta}^{\mathrm{f}} = \boldsymbol{\delta}(\phi)$, $\boldsymbol{\delta}^{\mathrm{s}} = \boldsymbol{\delta}(\phi, \boldsymbol{p})$, $\boldsymbol{\delta}^{\mathrm{a}} = \boldsymbol{\delta}(\phi, \boldsymbol{\theta})$ and $\boldsymbol{\delta}^{\mathrm{n}} = \boldsymbol{\delta}(\phi, \boldsymbol{\theta})$. With sampling-based methods (including INLA, which allows samples to be taken from the posterior), it is straightforward to obtain samples for $\boldsymbol{\delta}^{\mathrm{f}}, \boldsymbol{\delta}^{\mathrm{s}}, \boldsymbol{\delta}^{\mathrm{a}}, \boldsymbol{\delta}^{\mathrm{n}}$ using samples from $\phi, \boldsymbol{\theta}$, respectively.

Notes:

- For the multinomial within-year expected mortality model we use temperature only to account for seasonality of deaths. This is a simple model and so the month to month variation in the excess for the countries that use this model will not be as accurate as the cumulative yearly totals that use the observed mortality counts.
- For the subnational model, we emphasize that do not use any covariates.
- The above is slightly simplified, because in reality many countries switch between data types, such as having full data for part of the pandemic and then annual data only or no data. We could write down a more detailed posterior distribution but it would be complicated and no insight would be gained. As described in Section 4 of the main paper, we “benchmark" the join between full and no data, so that there are no sudden jumps.
- In a similar vein, China has subnational and annual national data, and we could write down the posterior, but it would not be useful.

Figure 1 summarizes, via a decision tree, how the models are chosen for the different types of data, and Figure 2 shows the relationship between the different models, and how they feed into the excess calculation.

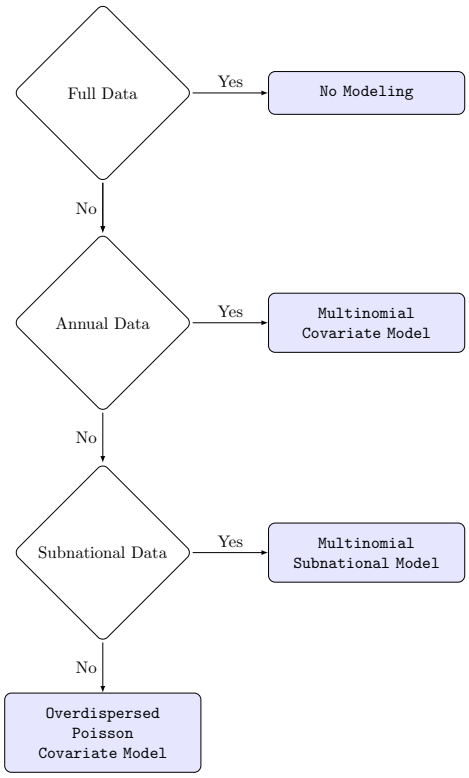

FIG 1. *Flowchart of ACM model choices based on data availability. The bottom box corresponds to the "No Data situation".*

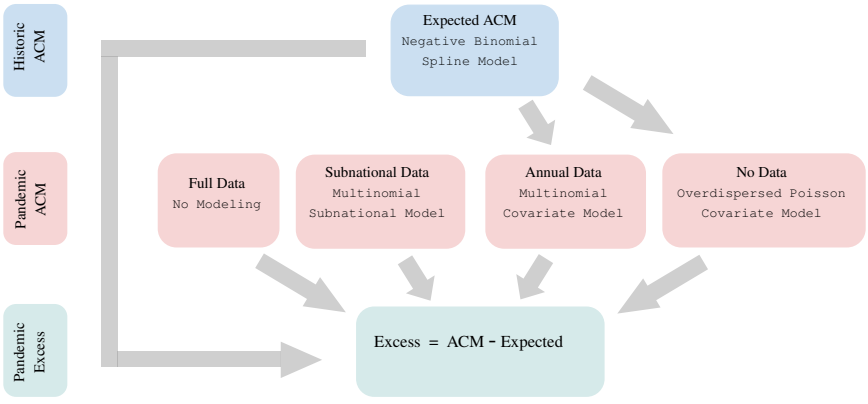

FIG 2. *Overview of modeling strategy.*

2. Supplementary Materials: Evidence from Countries without All-Cause Mortality Data. We briefly review preliminary evidence from researchers, journalists and various officials of significant excess mortality in many of the countries for which we have no ACM data. This includes, but is not limited to, evidence from Honduras (EFE, 2021), Haiti (DeGennaro *et al.*, 2021), Pakistan (Kirmani *et al.*, 2020), Tanzania (Parkinson, 2021), Bangladesh (Hanifi *et al.*, 2021; Rahman *et al.*, 2021a,b), Zambia (Mwananyanda *et al.*, 2021; Hamukale *et al.*, 2021), Syria (Watson *et al.*, 2021), Yemen (Besson *et al.*, 2021), Sudan (News, 2020; Moser *et al.*, 2021) and Papua New Guinea (Jorari, 2021). Also, evidence from territories which are not member countries show significant excess that tracks reported COVID-19 deaths. These territories neighbor many countries for which we lack data and are suggestive of similar patterns in their regions. This includes territories in the Pacific such as New Caledonia and French Polynesia, in the Caribbean such as Aruba, Guadeloupe, Martinique and Guadeloupe, and in Africa such as Réunion and Mayotte (Karlinsky and Kobak, 2021).

3. Supplementary Materials: Poisson-Multinomial Trick. Multinomial data cannot be directly fitted in INLA but can be modeled using the Poisson-Multinomial trick (Baker, 1994). For the multinomial model we use in Section 3.4 of the paper we can fit the Poisson model:

$$Y_{c,v,m}|\lambda_{c,v},\beta \sim \text{Poisson}(\lambda_{c,v}\exp(z_{c,v,m}\beta)),$$

with the default prior (normal distribution with large variance) for β and the improper prior $1/lambda_{c,v}$ for $\lambda_{c,v}$. We let $g_{c,v,m} = g_{c,v,m}(\beta) = \exp(z_{c,v,m}\beta)$ and $G_{c,v} = \sum_{m'} g_{c,v,m'}$. Then

$$\begin{aligned}
\Pr(\boldsymbol{Y}|\beta) &= \prod_c \prod_v \int \prod_m \exp(-\lambda_{c,v} \times g_{c,v,m})(\lambda_{c,v} g_{c,v,m})^{y_{c,v,m}} \times \lambda_{c,v}^{-1}\, d\lambda_{c,v} \times g_{c,v,m}^{y_{c,v,m}} \\
&\propto \prod_c \prod_v G_{c,v}^{-y_{c,v,+}} \prod_m g_{c,v,m}^{y_{c,v,m}} \\
&= \prod_c \prod_v \prod_m \left(\frac{g_{c,v,m}}{G_{c,v}}\right)^{y_{c,v,m}},
\end{aligned}$$

i.e., a multinomial with probabilities $g_{c,v,m}/G_{c,v}$, which is the model we wish to fit.

4. Supplementary Materials: Subnational Model Simulation Study. To examine the behavior of the Multinomial model that we use for subnational modeling in Section 5.1 of the paper, we perform a simulation study. We simulate ACM national data in month t from the model

$$Y_{+,t} = 1000 + 0.1 \times [1 + \sin(W_t)],$$

for $t = 1, \ldots, 24$ where $W_t = 0, \frac{\pi}{6}, \frac{\pi}{3}, \ldots, 4\pi$. Then from this underlying true total mortality we simulate subnational counts for $K = 5$ regions from our Multinomial model where,

$$\boldsymbol{Y}_t|\boldsymbol{p}_t \sim \text{Multinomial}_{K+1}(Y_{t,+}, \boldsymbol{p}_t),$$

with $\boldsymbol{p}_t = \{p_{t,k}, k \in S\}$,

$$p_{t,k} = \Pr(\text{ death in region } k \mid \text{period } t, \text{death }),$$

and

$$\log\left(\frac{p_{t,k}}{p_{t,K+1}}\right) = \alpha_k + \epsilon_t,$$

where the error term is given by $\epsilon_t \sim \text{N}(0, 0.5^2)$ and the α_k parameters are given in Table 2.

	Region 1	Region 2	Region 3	Region 4	Region 5
α_k	-0.25	-1.3	-1.15	-2.5	1.75

TABLE 2
Values of α_k used in the simulation study for the subnational model, $k = 1, \ldots, 5$.

Next, we randomly sample a number J of region-time points to remove as missing subnational values, to replicate a random pattern of missingness, similar to what we see in the subnational data for India. We choose $J = 20$ region-time observations, from the available total of $24 \times 5 = 120$. Finally, we fit the multinomial model described above using this data with the first $t = 1, \ldots, 18$ time points as observed subnational and total national mortality for fitting the model, and the remaining $t = 19, \ldots, 24$ time points for prediction and validation.

We then compare the predicted values from this subnational model to the true values of $Y_{+,t}$ which are known in this simulation setting.

In Figure 3, we show the data that are available, along with the predictions and truth in the final 6 time periods. In Figure 4, we show the observed national ACM in the last 6 months, along with the point and interval estimate from our model. The model captures the trend in the mortality well, though the interval estimates are quite wide.

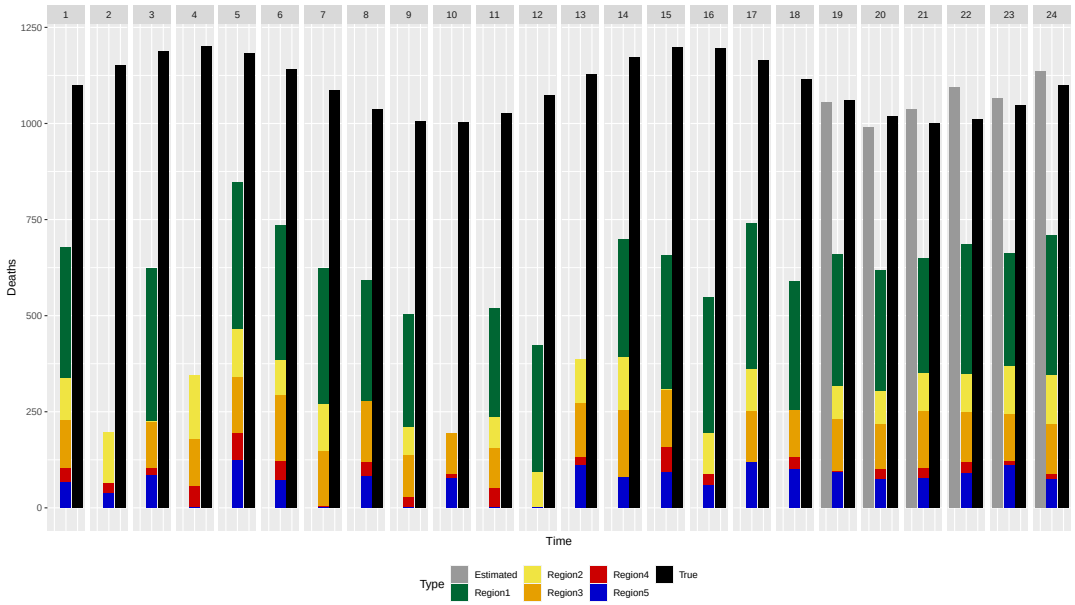

FIG 3. *Simulated regional and national data across all 24 time points, with the last 6 time points showing the estimated and true deaths.*

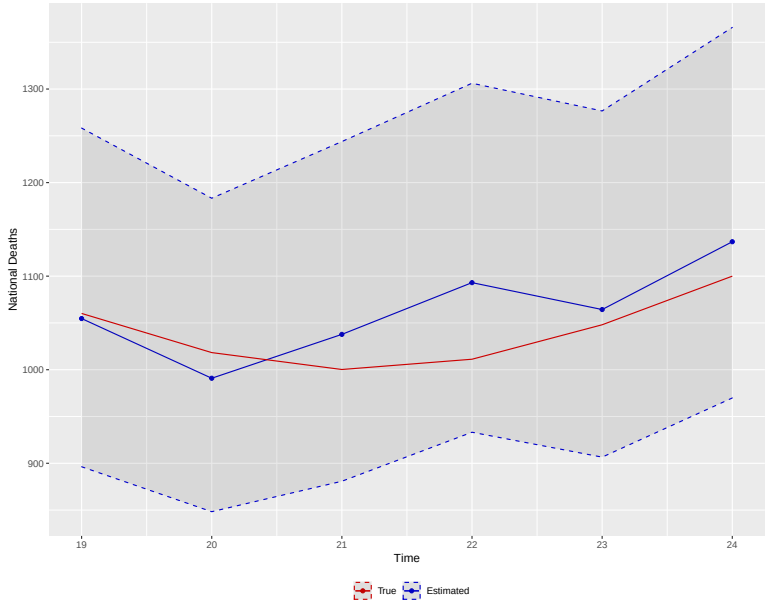

FIG 4. *Subnational simulation: True and predicted national deaths during the prediction window (6 time points), along with 95% credible interval.*

5. Supplementary Materials: Gamma Expected Numbers. In Section 3 of the paper we describe how the expected numbers are modeled using a negative binomial spline model. From this model we obtain Monte Carlo samples from the predictive distribution of the expected numbers in pandemic months. Note that we obtain the predicted for the mean count (so that we do not include negative binomial uncertainty). We approximate the distribution of the Monte Carlo samples using gamma distributions, which can then be marginalized over in our predictive log-linear Poisson model (since they are conjugate) – see Section 4 of the main paper for details.

In Figure 5 we show the gamma fits to the predicted distribution of the expected numbers, in December 2021, for a selection of countries. The differences between the predictions and the gamma approximations are small in all cases. This is a randomly chosen month, and is representative of the accuracy of the approximation.

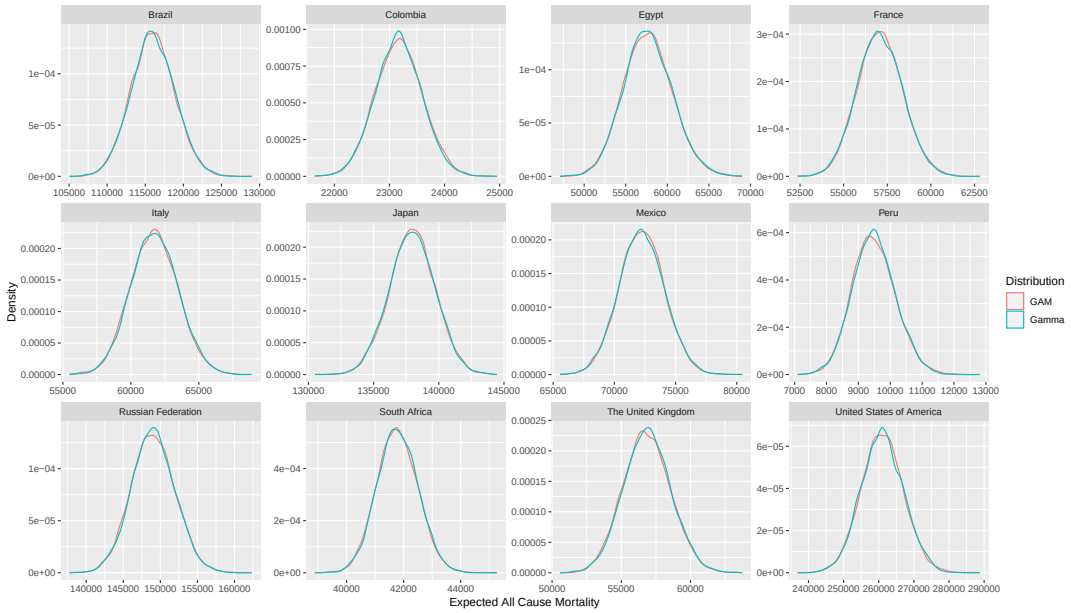

FIG 5. *Gamma fits to the predictive distributions of the expected numbers, for a range of countries, in December 2021.*

6. Supplementary Materials: Further Results.

6.1. *Global Summaries.* We first discuss the estimates for the association parameters in the log-linear model described in Section 4 of the paper:

$$\log \theta_{c,t} = \alpha + \sum_{b=1}^{B} \beta_{bt} X_{bct} + \sum_{g=1}^{G} \gamma_g Z_{gc} + \epsilon_{c,t}. \tag{1}$$

Apart from the high income indicator, all covariates are standardized to have mean 0 and standard deviation 1, which aids in prior specification and when comparing estimated coefficients. This should be borne in mind as associations are examined.

We first look at empirical univariate associations. We model the temperature association as time-varying and so in Figure 6 we plot $\log(Y_{c,t}/E_{c,t})$ versus temperature $x_{c,t}$ (for countries with observed data) and for each month $t = 1, \ldots, 24$. Starting with the simpler model $Y_{c,t}|\theta_{c,t} \sim \text{Poisson}(E_{c,t}\theta_{c,t})$ we derive the variance for $\log(Y_{c,t}/E_{c,t})$ as proportional to $Y_{c,t}^2/E_{c,t}$ and we take the reciprocal of this in a weighted least squares analysis. In Figure 7, we plot the exponentiated slopes from simple linear models fitted to each month, to give an indication of the associations. We see a clear time-varying association. The pattern is consistent with the bottom left panel of Figure 16, where the exponentiated fit from the overdispersed Poisson model is shown, albeit smoothed which is induced by the RW2 prior on the log relative rates associated with temperature.

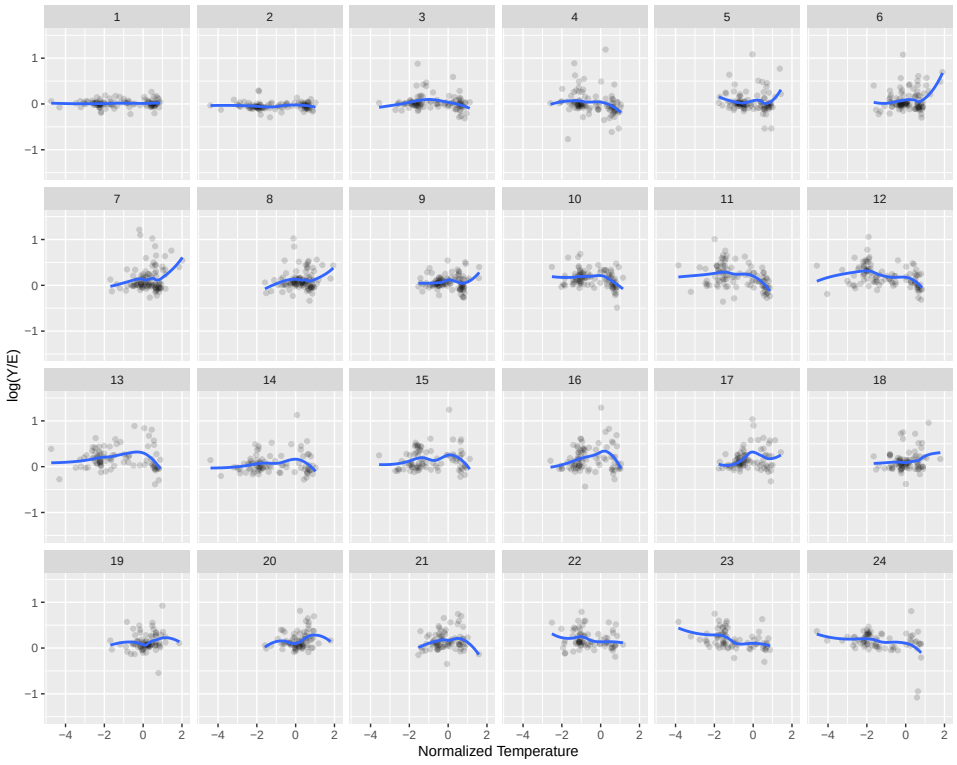

FIG 6. *Association between* $\log(Y/E)$ *by month and temperature, with smoothers.*

In Figures 8 and 9 we see the time-varying associations with the sqrt COVID-19 death rate, for high income and low/middle income countries. The associations are strong and the

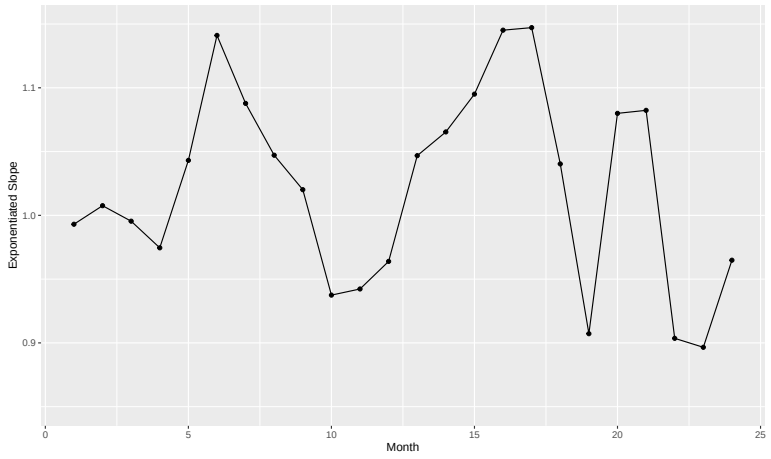

FIG 7. *Estimates of relative rate parameters associated with temperature, by month.*

smoothed versions from the full covariate model can be seen in the top right panel of Figure 16.

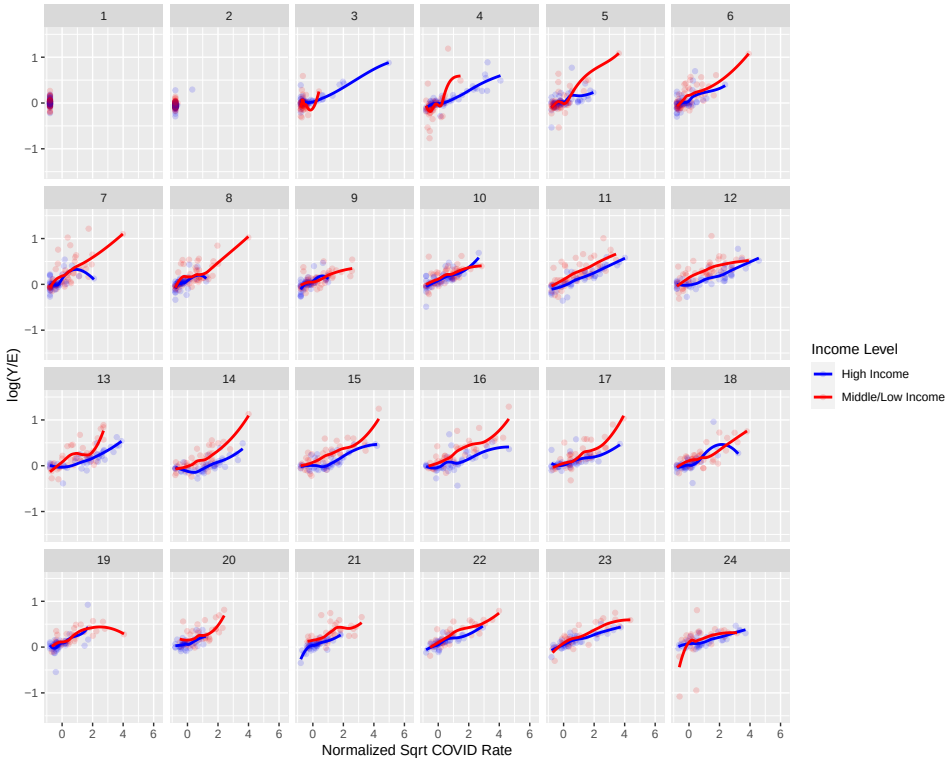

FIG 8. *Association between* $\log(Y/E)$ *by month and sqrt COVID-19 death rate, with smoothers.*

Figures 10 and 11 show the COVID-19 positive test associations, and we see similar and positive though weak associations in both income groups.

Figures 12 and 13 show the containment associations, and we see again similar and negative relationships in both income groups.

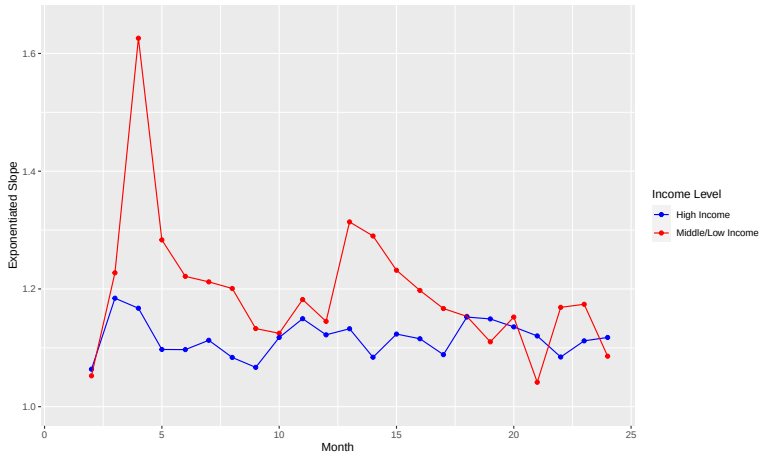

FIG 9. *Estimates of relative rate parameters associated with sqrt COVID-19 death rate, by month.*

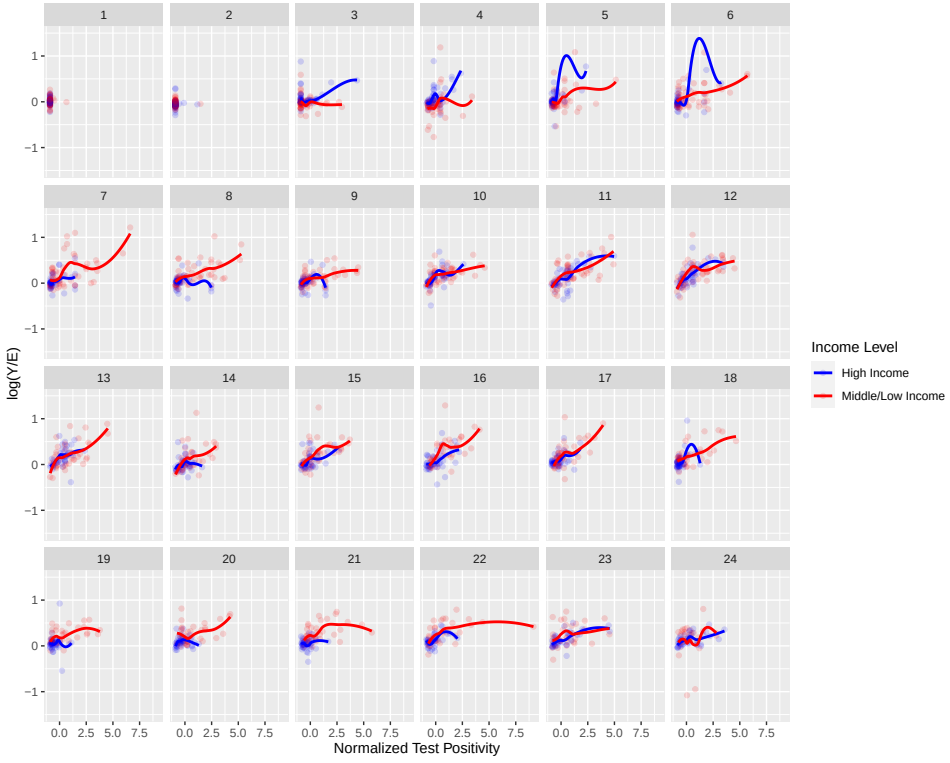

FIG 10. *Association between* $\log(Y/E)$ *by month and positive COVID-19 test rate, with smoothers.*

Finally, the two constant covariate associations are given in Figure 14. A high historic diabetes rate is associated with a lower rate. Figure 15 summarizes the fixed effects. In general, for the variables with interactions, the associations are stronger and the intervals narrower, for low/middle income countries, where the pandemic produced more excess deaths (see Figure 18).

In Figure 15 we summaries the fixed effect parameters – we parameterize the model so that the time-varying associations have an overall (average) association and then variation around

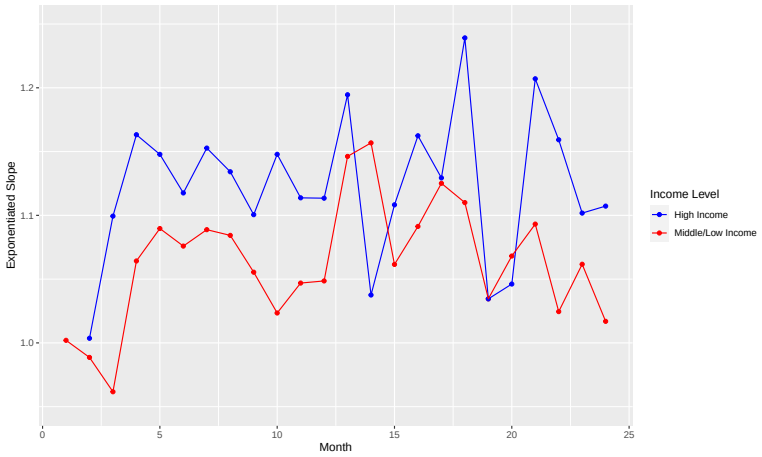

FIG 11. *Estimates of relative rate parameters associated with positive COVID-19 test rate, by month.*

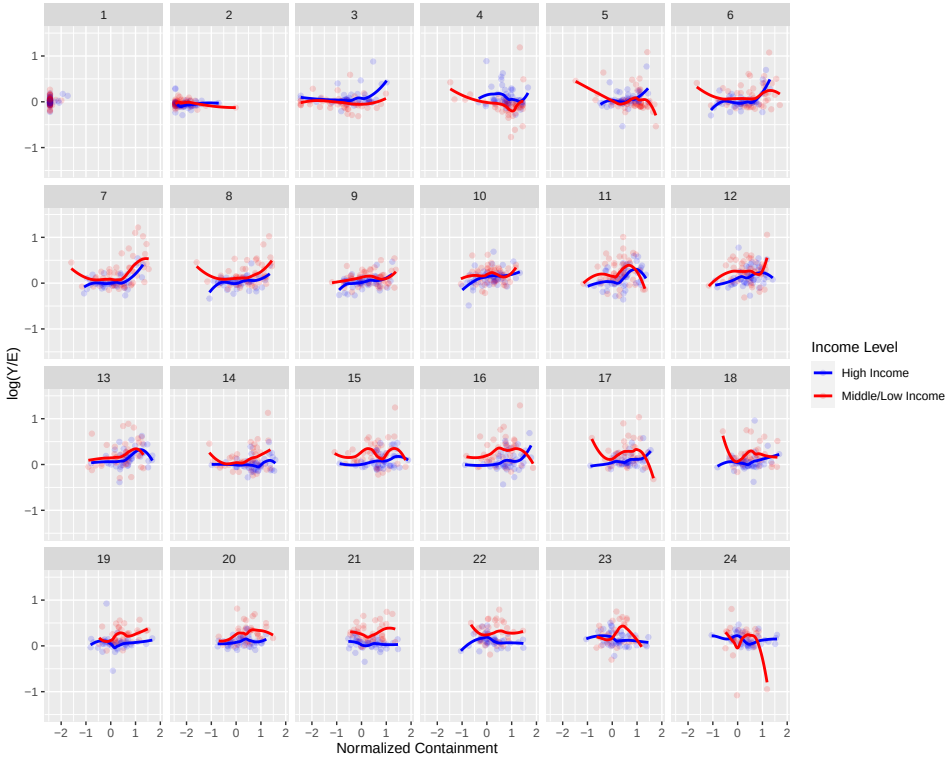

FIG 12. *Association between* $\log(Y/E)$ *by month and containment, with smoothers.*

this with a RW2 (with a sum-to-zero constraint). The strongest association is with the sqrt COVID-19 death rate in low- and middle-income countries, in the expected direction. The test positivity rate in low- and middle-income countries is also positivity, as is the temperature association. The sqrt COVID-19 death rate in high-income countries is in the opposite direction to that expected. Containment in low- and middle-income countries has a negative association, as does the historic diabetes rate.

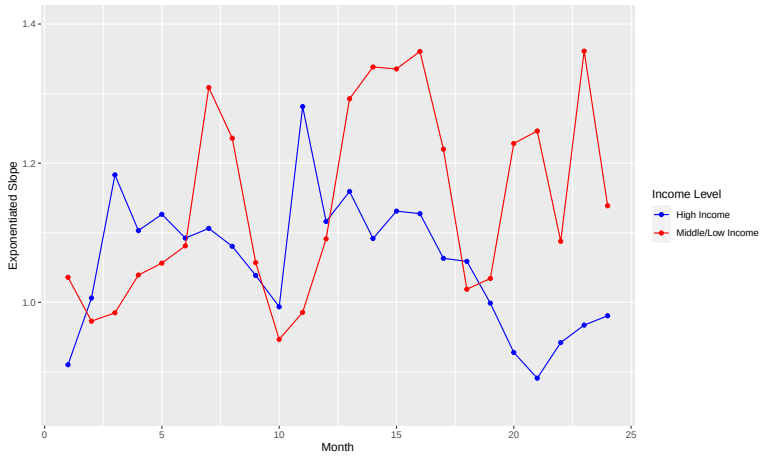

FIG 13. *Estimates of relative rate parameters associated with containment, by month.*

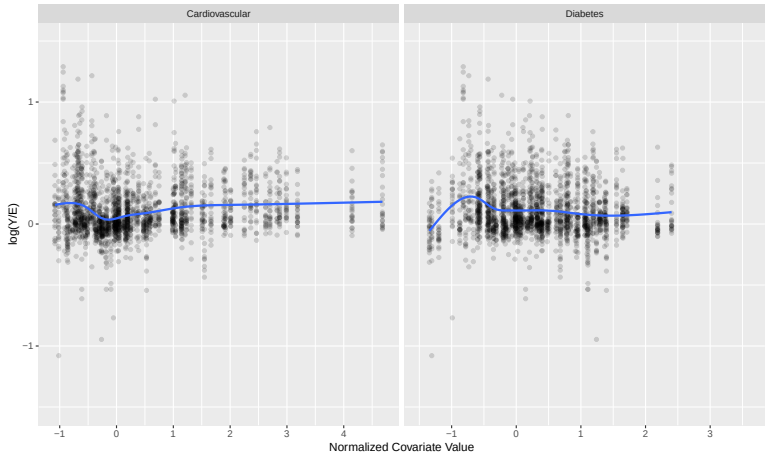

FIG 14. *Estimates of relative rate parameters associated with the time constant covariates, cardiovascular and diabetes rates from 2019.*

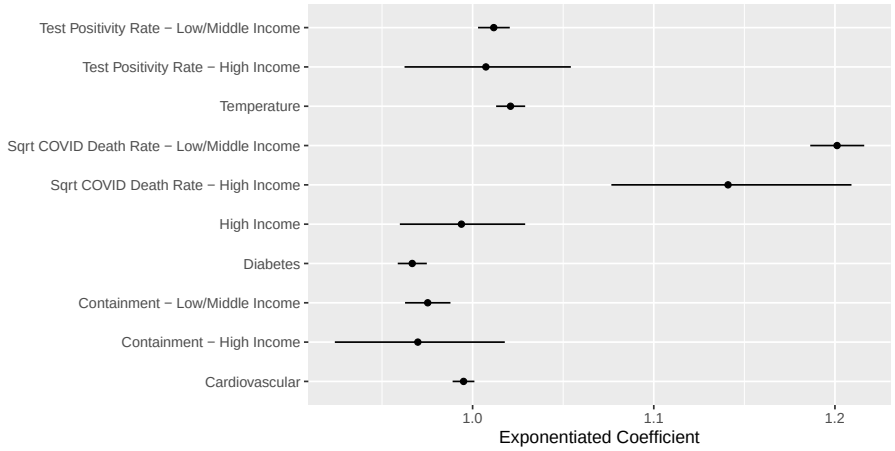

FIG 15. *Fixed association coefficients, with 95% interval estimates. We plot the multiplicative change in the relative rate of the excess associated with a 1-unit increase in the relevant covariate.*

The fitting of the covariate model to the monthly ACM data resulted in the association parameters in Figure 16. We see that the time-varying aspect seems merited in all cases, apart perhaps from test positivity which is relatively constant, and close to 1. We could have removed this covariate from the model, but we wanted to minimize model changes. The containment and test positivity follow qualitatively similar shape; initially the association is lower so that higher containment and test positivity rates are associated with a relatively reduced mortality rate, relative to that expected. And then, from July 2020, the associations are relatively constant.

We did consider models using lagged covariates, but the fits were similar to the ones shown here. We will continue to explore this issue in future extensions. In general, in future work we would like to investigate flexible yet principled model-building strategies, with an enhanced set of country-level variables.

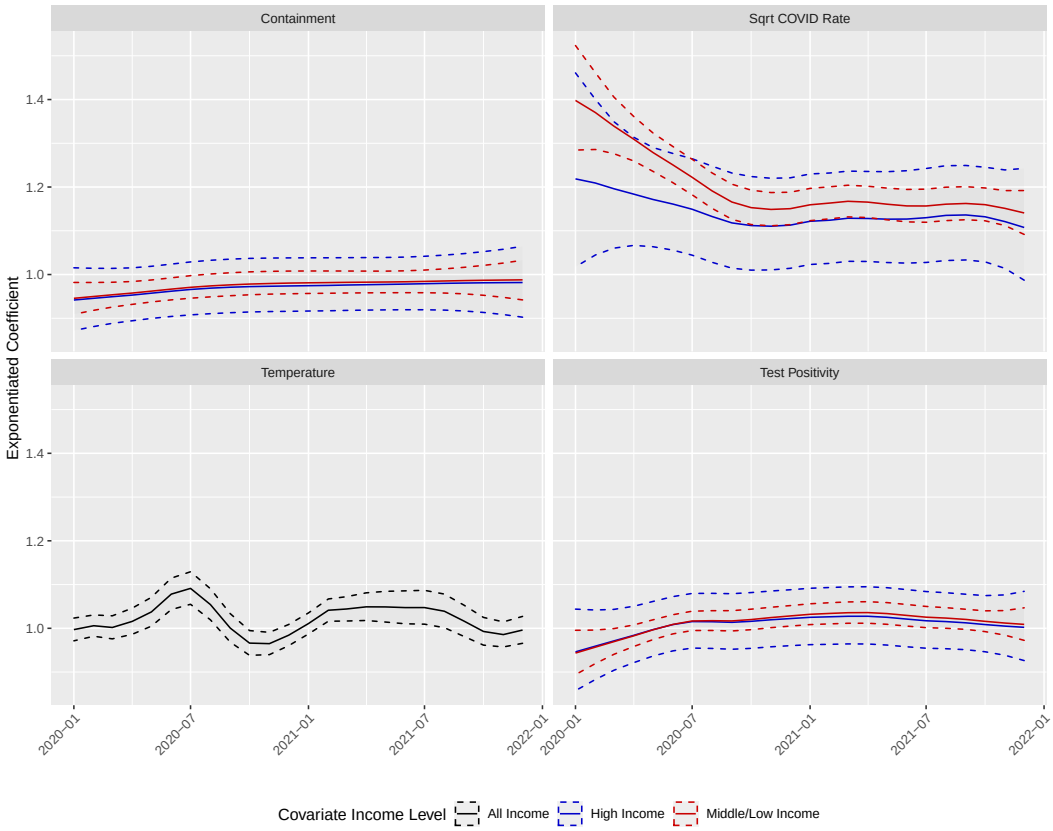

FIG 16. *Time-varying associations versus month, with 95% interval estimates. We plot the multiplicative change in the relative rate of the excess associated with a 1-unit increase in the relevant covariate, against month.*

Using samples from the posterior (available from INLA), we can obtain rankings of the countries, in terms of the excess mortality rate. We show these rankings in Figure 17. The posterior probability that Peru has the highest excess rate is very close to 1. Similarly, the second highest rank is for Bulgaria, again with high probability. From the 3rd highest on it is less definitive but Bolivia also clearly has a high excess rate, as do the Russian Federation, North Macedonia, Armenia and Montenegro. The posterior distribution for Saint Vincent and the Grenadines is very wide, and so its probabilities are sprinkled across the rankings. After the first two ranks, there is a lot of ambiguity in the rankings, showing that it is deceptive to simply rank in terms of a single posterior summary such as the median.

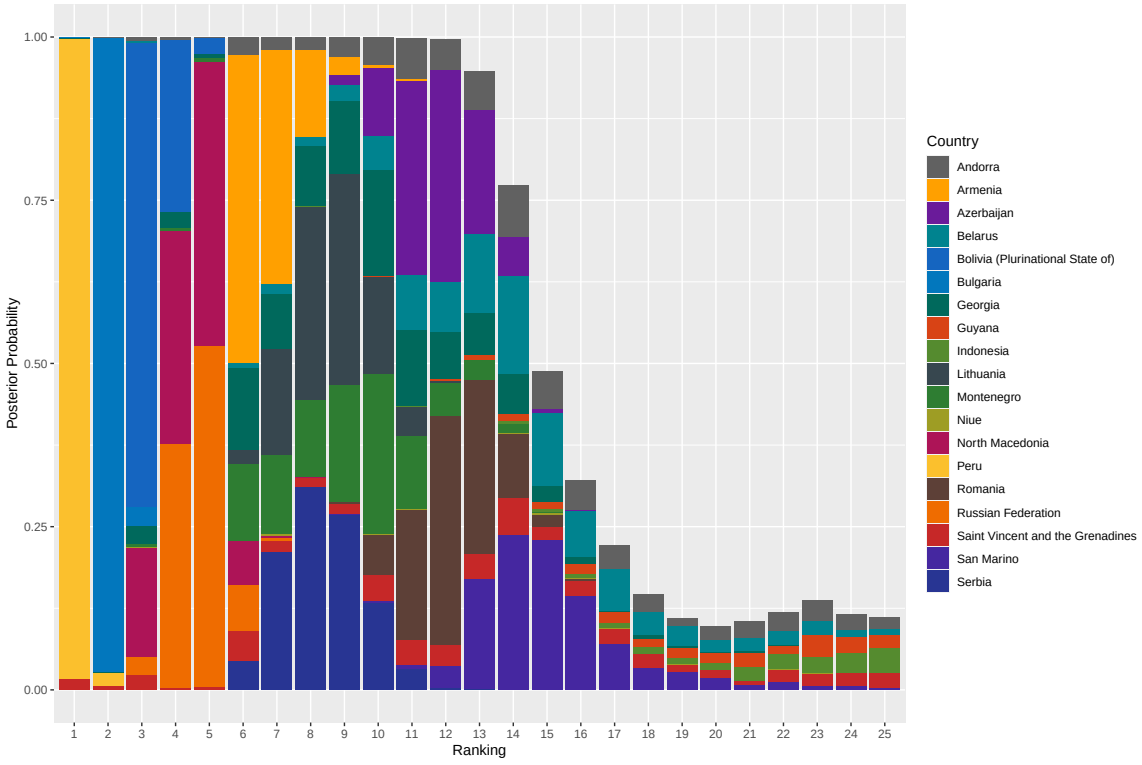

FIG 17. *Posterior probability of particular countries having high ranks for the greatest excess mortality rate.*

In Figure 18, we show the cumulative excess deaths, by income status. The majority of the excess deaths occur in low/middle income countries.

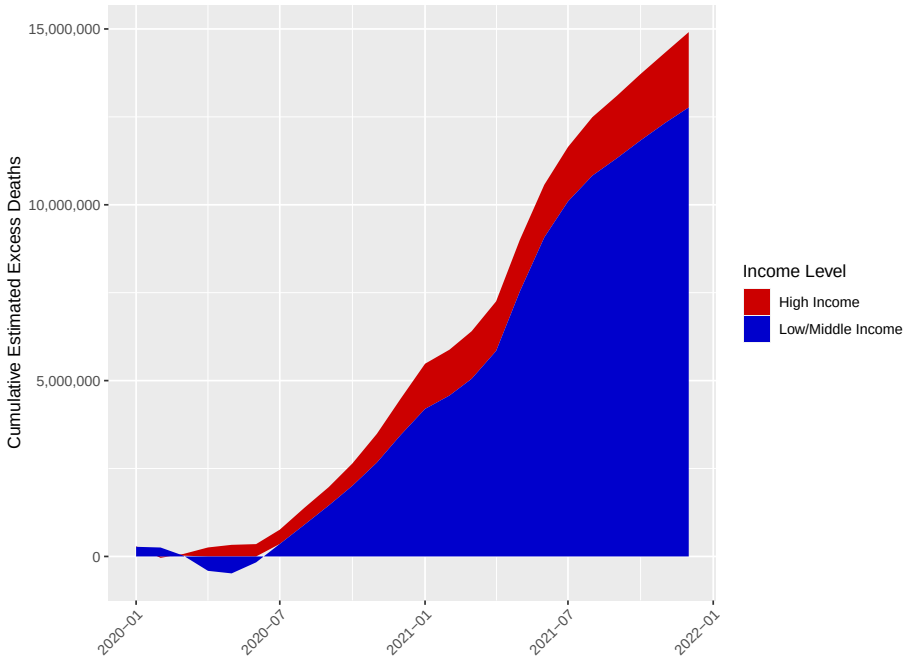

FIG 18. *Cumulative excess deaths over 2020–2021, by high and low/medium income.*

In Figure 19 we plot cumulative excess deaths over 2020–2021, by region. The most startling change is how large the SEARO contribution becomes, because of the addition of India.

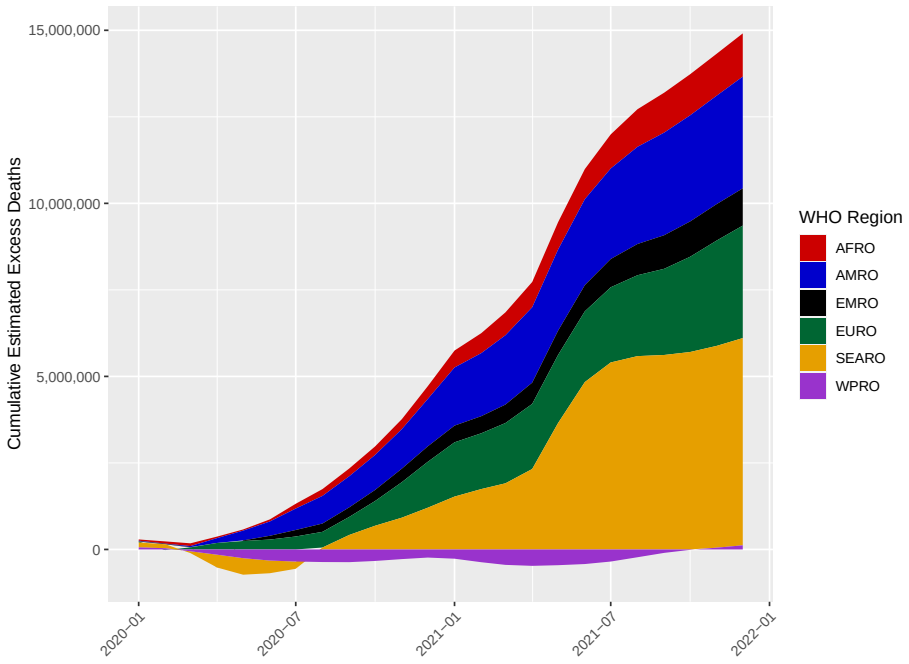

FIG 19. *Cumulative excess deaths over 2020–2021, by region.*

6.2. *Argentina.* We now describe each of the analyses carried out for countries with subnational data, starting with Argentina.

We first describe the available data. For 2019 and 2020, we have total national deaths and deaths in the province of Cordoba, both by month. For 2021, there are subnational data for Cordoba. In Figure 20 we plot the fraction of Cardoba deaths to national deaths in 2019 and 2020. There is some variation, and perhaps a small uptick in the fraction toward the end of 2020, but overall the fraction is quite constant, and there is not a drastic change in the first year of the pandemic, as compared to the previous year.

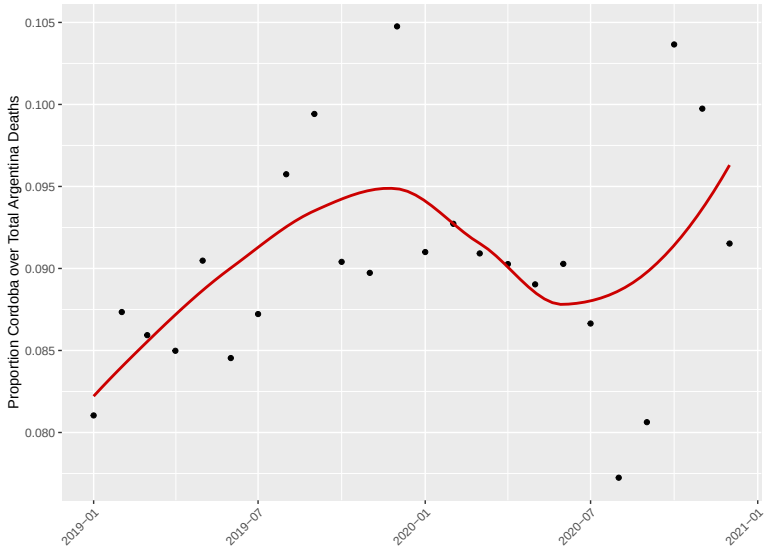

FIG 20. *Fractions of the total deaths in Cordoba, for 2019 and 2020, with smoother.*

In Figure 21 we plot the predictions for 2021 from the subnational binomial model and from the predictive covariate model which is estimated from the countries with national monthly data. There are some differences between the results, with the covariate model giving wider intervals and higher estimates from April 2020. In the reported results we use the subnational estimates.

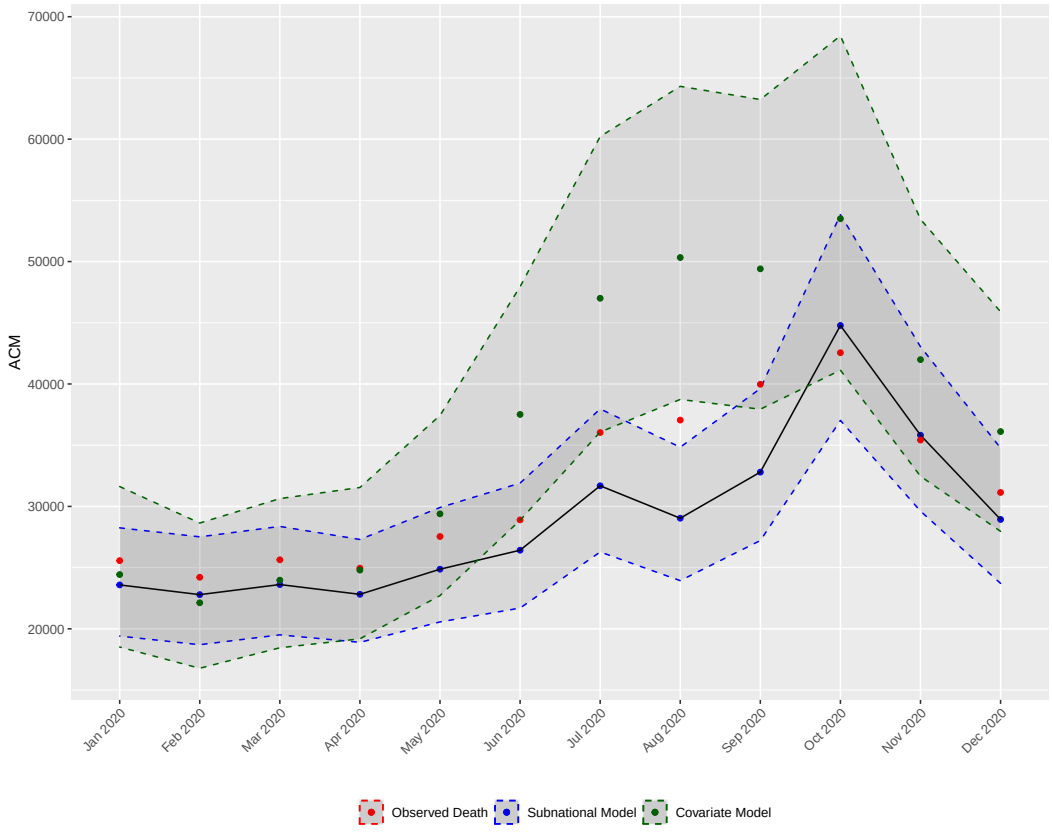

FIG 21. *Argentina national data and predictions. Predicted deaths from the subnational model, and from the global negative binomial covariate model for 2021, both with 95% credible intervals*

6.3. *China.* For China, we have two main data sources. First, the annual national ACM from 2015 to 2021, as reported by the National Bureau of Statistics of China in the 2021 statistical yearbook (National Bureau of Statistics of China, 2021) and a January 2022 press release (National Bureau of Statistics of China, 2022). Second, we may potentially utilize data on the daily number of deaths registered by the nationally representative Disease Surveillance Points (DSP) system in January–August 2019 and January–August 2020, as reported by Qi *et al.* (2022). The DSP registered about 18% of total deaths in China in 2019 (Zeng *et al.*, 2020) and we aggregate the DSP data to monthly national counts. The data collection sites are constant over time so that the fraction of the population covered is constant also. To use the subnational model described in Section 5.1 of the main paper we impute *monthly* national ACM counts, based on a 12-cell multinomial, conditioned on the *annual* national ACM, The monthly probabilities are modeled as a log-linear function of temperature, as we did in the modeling of the expected numbers (described in Section 3 of the main paper).

To make inference for this model we needed to write our own Markov chain Monte Carlo (MCMC) algorithm (the model is not of the form allowed in INLA, and it requires the generation of discrete counts, which cannot be done in `Stan`). We denote the apportioned counts in 2019 as the 12×1 vector $\boldsymbol{Y}^{2019}$, and treat as known (so that we ignore the fact that we imputed these counts). We let $\boldsymbol{z}^{2019}$ and $\boldsymbol{z}^{2020}$ represent the monthly DSP counts in years 2019 and 2020, and p_t be the fraction of deaths from the DSP in month t. We model p_t as, $\text{logit}(p_t) = \alpha + \epsilon_t$, with $\epsilon_t \sim \text{N}(0, \sigma_\epsilon^2)$ and let $\boldsymbol{a}^{2020}$ be the collection (across months) of fixed covariate predictions based on the global covariate model.

The unknown monthly ACM counts in 2020 are denoted $\boldsymbol{Y}^{2020}$. The posterior is,

$$p(\boldsymbol{Y}^{2020}, \alpha, \sigma_\epsilon^2 | \boldsymbol{z}^{2019}, \boldsymbol{z}^{2020}, \boldsymbol{Y}^{2019}, Y_+^{2020}, \boldsymbol{a}^{2020}) \propto p(\alpha, \sigma_\epsilon^2 | \boldsymbol{z}^{2019}, \boldsymbol{Y}^{2019}) \times p(\boldsymbol{Y}^{2020} | \alpha, \sigma_\epsilon^2, \boldsymbol{z}^{2019}, \boldsymbol{z}^{2020}, Y_+^{2020})$$

An MCMC scheme alternates between sampling from the conditionals for p and for $\boldsymbol{Y}^{2020}$. The conditional for $\alpha, \sigma_\epsilon^2$ is

$$\begin{aligned} p(\alpha, \sigma_\epsilon^2 | \boldsymbol{z}^{2019}, \boldsymbol{Y}^{2019}) &\propto p(\boldsymbol{z}^{2019} | \alpha, \sigma_\epsilon^2, \boldsymbol{Y}^{2019}) \\ &\sim \prod_{t=1}^{8} \text{Binomial}(Y_t^{2019}, p_t) \times \pi(\alpha)\pi(\sigma_\epsilon^2), \end{aligned}$$

where $p_t = p_t(\alpha, \sigma_\epsilon^2)$. The conditional for $\boldsymbol{Y}^{2020}$ is more involved:

$$p(\boldsymbol{Y}^{2020} | \alpha, \sigma_\epsilon^2, \boldsymbol{z}^{2019}, \boldsymbol{z}^{2020}, Y_+^{2020}, \boldsymbol{a}^{2020}) \propto \underbrace{p(\boldsymbol{z}^{2020} | \boldsymbol{Y}^{2020}, \alpha, \sigma_\epsilon^2)}_{\text{Product of Binomials}} \times \underbrace{p(\boldsymbol{Y}^{2020} | Y_+^{2020}, \boldsymbol{a}^{2020})}_{\text{Multinomial}}$$

For the proposal for the vector $\boldsymbol{Y}^{2020}$ we need to ensure that the total Y_+^{2020} is respected. The MCMC algorithm we use, is in the spirit of algorithms described in Wakefield *et al.* (2011), and is given by:

1. Draw K from a discrete distribution on $1, 2, \ldots, 6$.
2. Draw K counts. Decrease these counts by some fixed discrete number J.
3. Draw K of the remaining counts. Increase these counts by J.
4. Together with the counts we do not sample, we therefore form a new set of counts with the same total.

We first report a simulation study in which we validate the MCMC sampling for the prediction of monthly country ACM from reported annual ACM and monthly subnational ACM. We conceived the following setup where we simulate,

$$Y_{+,t} = \text{Unif}(5000, 20000)$$

with $t = 1, \ldots, 12$ as the true unobserved total monthly ACM and where we have the observed annual total $\sum_{t=1}^{12} Y_{+,t}$ and the observed subnational ACM given by,

$$z_t = Y_{+,t} \times p_t$$

where logit $p_t = -1.5 + \epsilon_t$ with $\epsilon_t \sim \mathrm{N}(0, 0.1)$. We also simulate our covariate model outcomes as $a_c = Y_{+,t} + \delta_t$ with $\delta_t \sim \mathrm{N}(0, 0.05 \times Y_{+,t})$ and where the error has variance fractionally larger than the percent relative error of the covariate model. Following this simulation scheme for the data, through the MCMC sampling approach outlined above and initializing using $Y_{+,t}/12$ for each cell count, we run 10,000 iterations. We obtain monthly estimates that stabilize around the true values $Y_{+,t}$ as shown in Figure 22, following an acceptance rate that stabilizes just below 0.50 as shown in Figure 23.

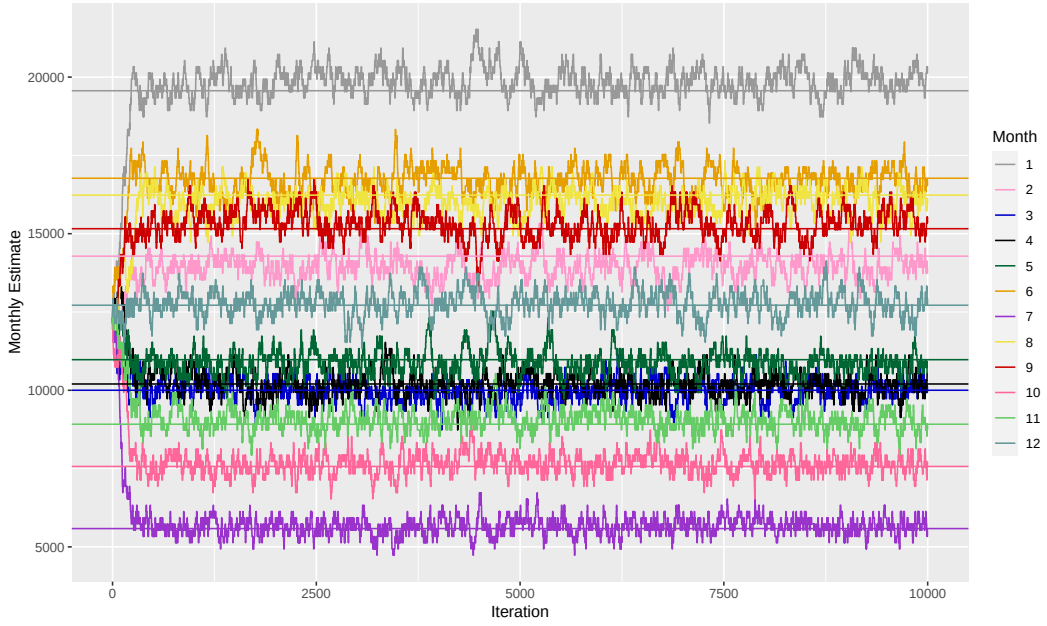

FIG 22. *Estimated monthly ACM across all 12 time points where the horizontal lines display the true monthly simulated ACM.*

There are reasons to believe that the China DSP system may have become less reliable during the pandemic (Haidong Wang, personal communication), and so we carry out two analyses, one in which we apportion out the annual ACM counts using the DSP data and covariate prior, and the other in which we use the covariate prior only.

In Figure 24, we plot the expected numbers, with uncertainty, along with the predictions based on the covariate model only (2020–2021), and the covariate model plus subnational data (2020). The 2020 estimates are very similar under the two approaches, which is reassuring. For the final reported numbers, we used the covariate model, given the aforementioned question mark over the accuracy of the DSP data.

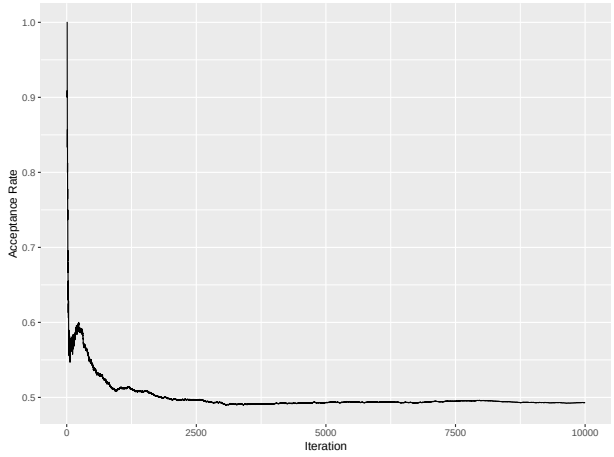

FIG 23. *Cumulative acceptance rate of proposed monthly ACM vector across iterations within the MCMC chain.*

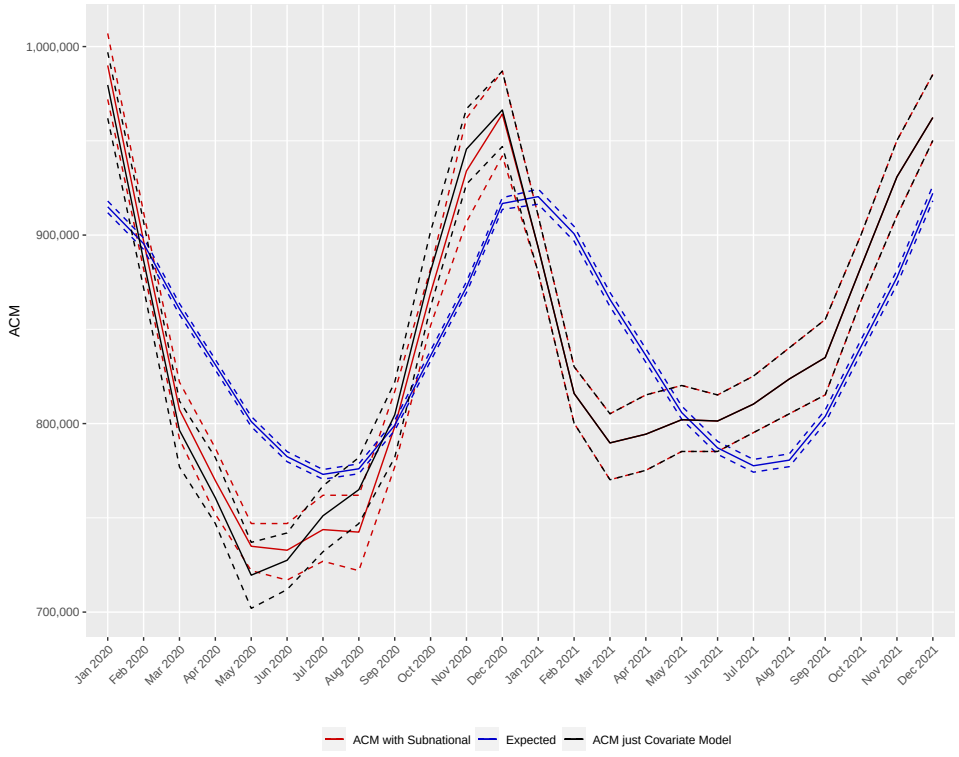

FIG 24. *Expected numbers for China, along with within-year predictions based on: covariate model only, covariate model and subnational data.*

6.4. *India.* For India, we use a variety of sources for registered number of deaths at the state and union-territory level. Some information was reported directly by the states through official reports and automatic vital registration:

Karnataka Birth and Death Registration (URL data 2022-03-05):
`https://ejanma.karnataka.gov.in/frmTransaction_Details.aspx`

Kerala Civil Registrations (URL date 2022-03-05):
`https://cr.lsgkerala.gov.in/Pages/Map.php`

Birth and Death Odisha (URL date 2022-03-05):
`https://www.birthdeath.odisha.gov.in/#/home`

Tamil Nadu Births and Deaths (URL date 2022-03-05):
`https://www.crstn.org/birth_death_tn/MisRep.jsp`

We also used data obtained by journalists who obtained death registration information through Right To Information requests: Rukmini (2022a); Saikia (2022); NDTV.com (2022); Ramani and Radhakrishnan (2021); Ramani (2021a,f,b); Rukmini (2022b); Ramani (2021c); Ramani and Vasudeva (2021b); Ramani (2021d); Staff (2022); Ramani (2021e); Ramani and Vasudeva (2021a); The Times of India (2021). Some of the state level data before and during the pandemic was scaled up to account for incomplete registration where vital registration captures only some of the deaths that occur, as shown in Office Of The Registrar General (2021). For the historic national totals, the WHO takes the Civil Registration System (CRS) data provided by the Indian government; the CRS is implemented by the Office of the Registrar General of India (ORGI) housed in the Ministry of Home Affairs, under the Registration of Births and Deaths Act, 1969.

It is known that the CRS suffers from under-reporting. Rao and Gupta (2020) report that completeness of death registration from 67% in 2011 to 79% in 2017. The WHO adjusts the CRS data for under-reporting, using a method that uses life tables and data from the Indian Sample Registration System (SRS) which is a random sample of under 1% of the national population (WHO, 2020). In Figure 25 we plot the completeness by year, along with the completeness we assume for 2020 and 2021 (we use the last completeness estimate).

Figure 26 displays the reported deaths by those states that we have data for during the pandemic.

For the final 3 months of 2021 there are data available from a single state only (Tamil Nadu) available, and for these 3 months the counts appear high (perhaps due to late registration), and so we do not use these data and instead use a simple predictive model. Specifically, we model $\log(Y_t/E_t)$ (using the estimated Y_t for the first 21 months and weighting by the variance of the estimate) using an autoregressive order 1 (AR1) model in INLA (we experimented with various choices, including splines and RW1 and RW2 models), and then predict the final 3 months. Figure 27 shows various summaries from the AR1 model. We wanted predictions for last 3 months that were relatively neutral, since we have not seen any evidence to suggest large changes in India in this period.

Figure 28 shows the predicted ACM for India, based on the state level data, along with the expected deaths, both with credible intervals.

Figure 29 shows the ACM counts by states, and the remainders, which sum to the total ACM, by month. Figure 30 shows the pandemic period, with the crucial change being that now the black rectangles are estimated, based on the fraction of deaths in each state, as

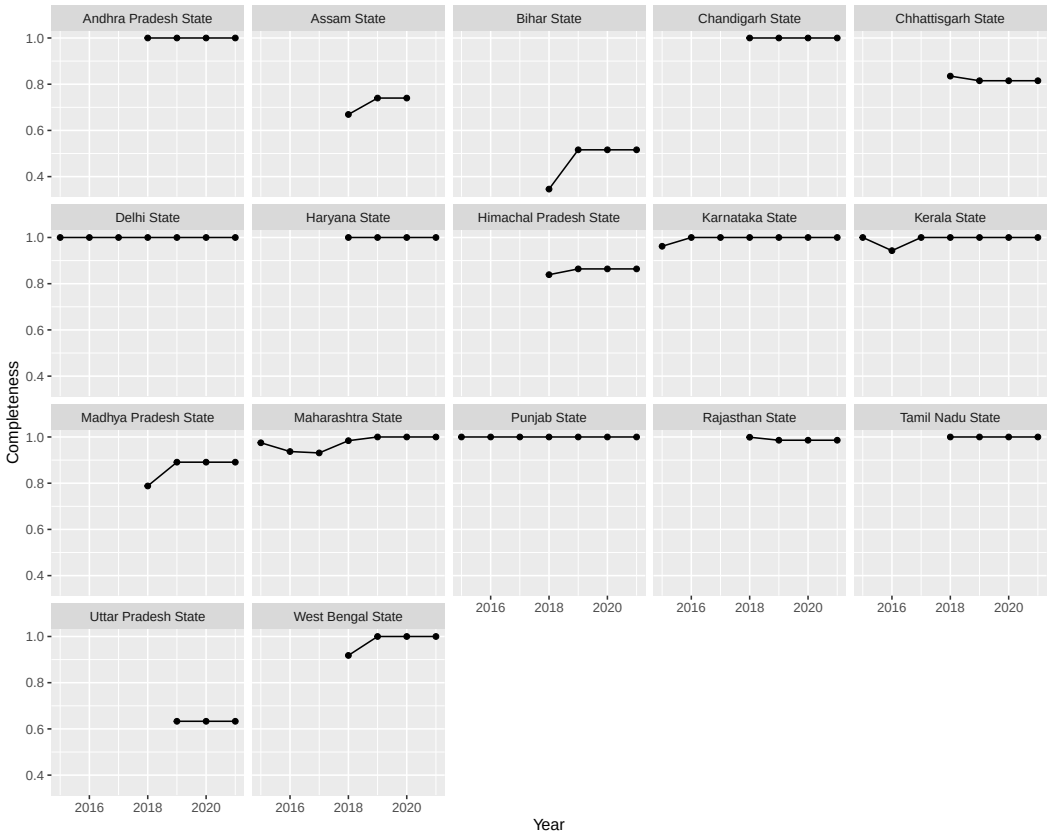

FIG 25. *Completeness for the 17 states for which we have subnational data during the pandemic.*

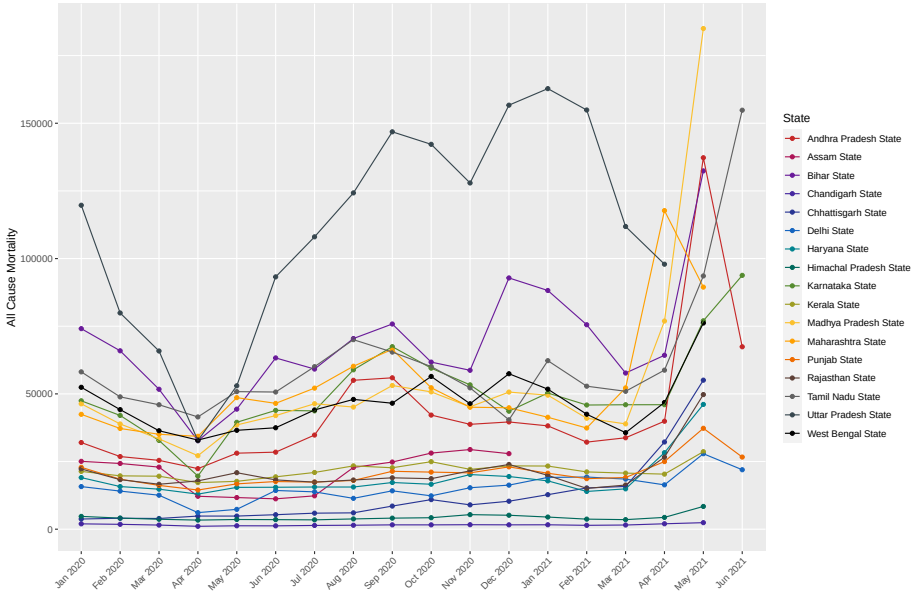

FIG 26. *Plot of reported deaths by Indian States.*

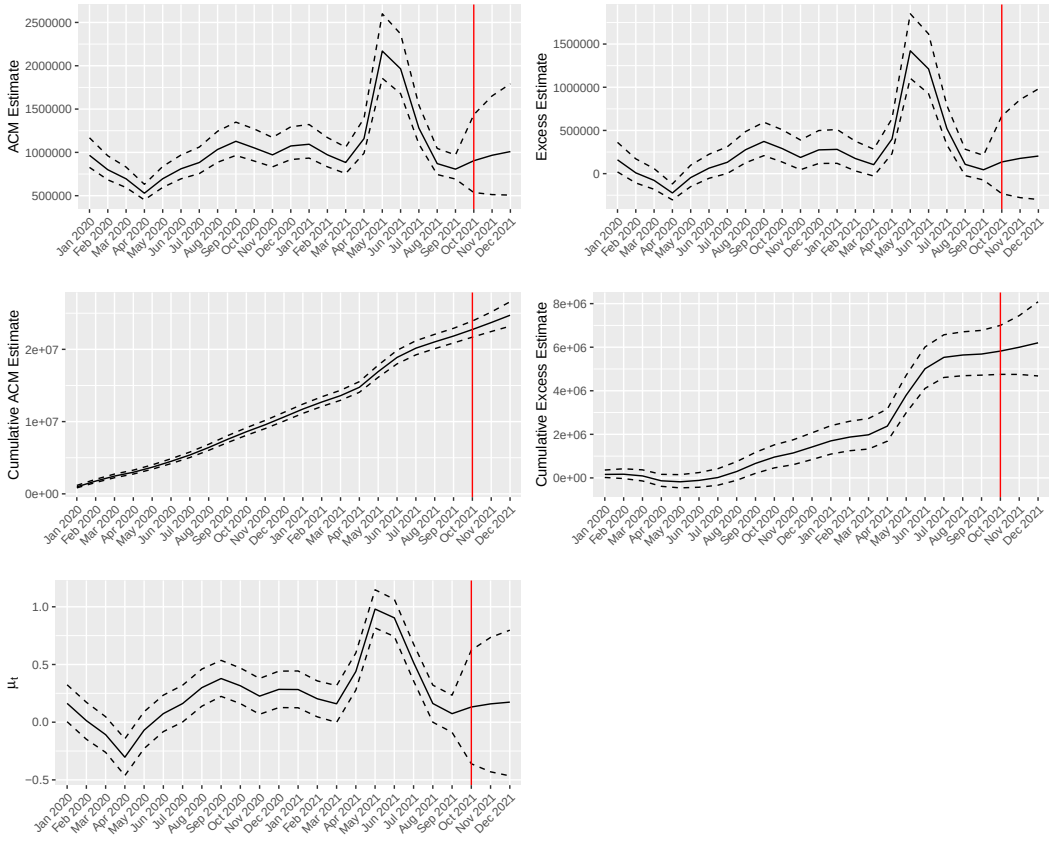

FIG 27. *AR1 prediction model for India. In the bottom left we plot the AR1 contribution.*

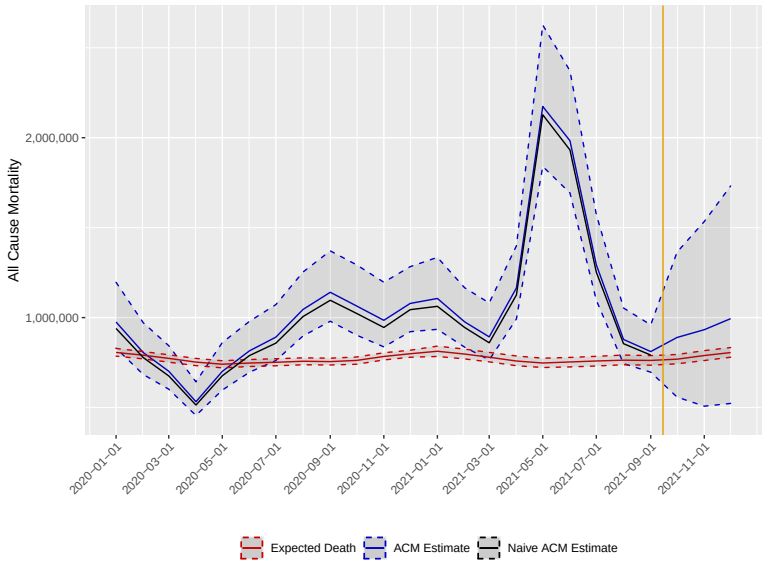

FIG 28. *Estimates with 95% uncertainty for India. The final 3 months are based on an AR1 model.*

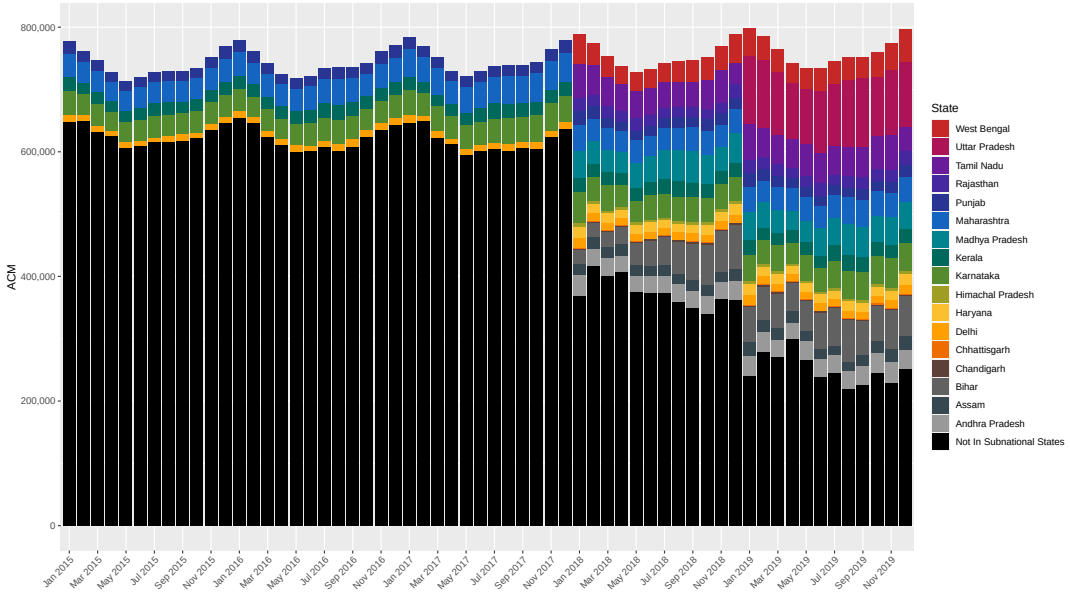

FIG 29. *All-cause mortality by month in pre-pandemic period, 2015–2019. Black rectangles are totals while colored rectangles are the states for which we have data in the pandemic.*

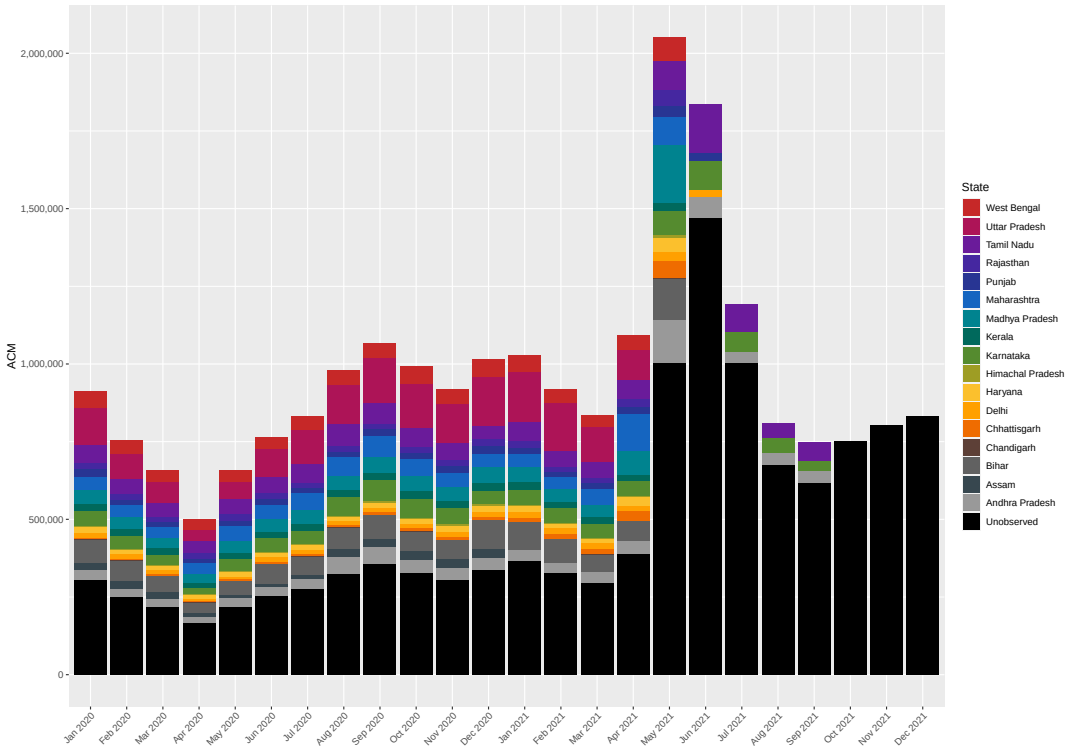

FIG 30. *All-cause mortality by month in the pandemic. Black rectangles are estimated while colored rectangles are observed.*

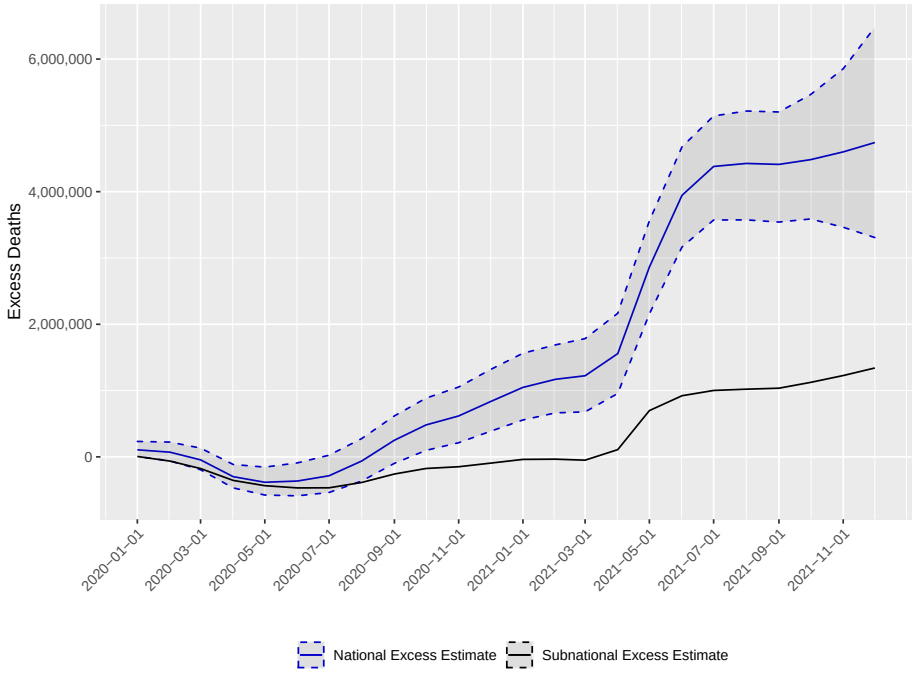

FIG 31. *Cumulative excess over January 2020 to December 2021. The black curve is the contribution from the observed state level data.*

estimated from the data in Figure 29. Figure 31 shows the cumulative excess over January 2020–December 2021, along with the estimated contribution from the state-level data only.

Recall that the subnational model is built on the assumption that the proportion of deaths in a state is approximately constant over time. Having data from many states does protect from requiring a constant fraction assumption for all states, since the level of bias depends on the cumulative effects of departures from constancy across all states.

To address the sensitivity we carried out analyses based on different subsets of the data and estimating the fractions of deaths based on data from 2015–2019, or from 2019 only. Figures 32 and 33 show the time series of estimated national ACM for different subsets of states, and based on different years of subnational data. Figures 34 and 35 show the cumulative national ACM versions of these plots. For monthly and cumulative plots we split into two sets to make the plots simpler to read. The cumulative totals are substantively similar, offering evidence that the excess result is not being driven by data from any one state.

To further assess the Indian subnational model, we carry out the following leave-one-out strategy. We systematically leave one state out at a time, and then estimate the monthly national distribution of ACM, by month. We then apply the estimate of the fraction of the left out state to the total, and compare with the observed ACM. Figures 36 and 37 show the resultant time series and cumulative totals. The predictions are better for some states than others but they are not systematically higher or lower, which gives some reassurance that our model is robust. Chandigarh is low and Chhattisgarh is high, but these states are responsible for a small proportion of the total.

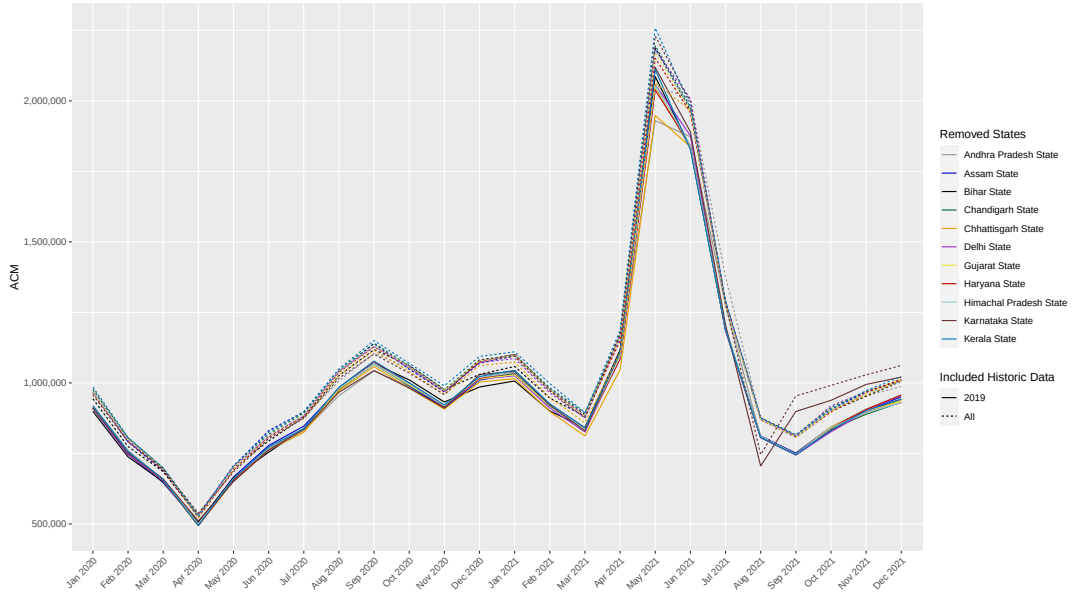

FIG 32. *Time series of ACM with different states excluded, and with different years of data used for the expected numbers.*

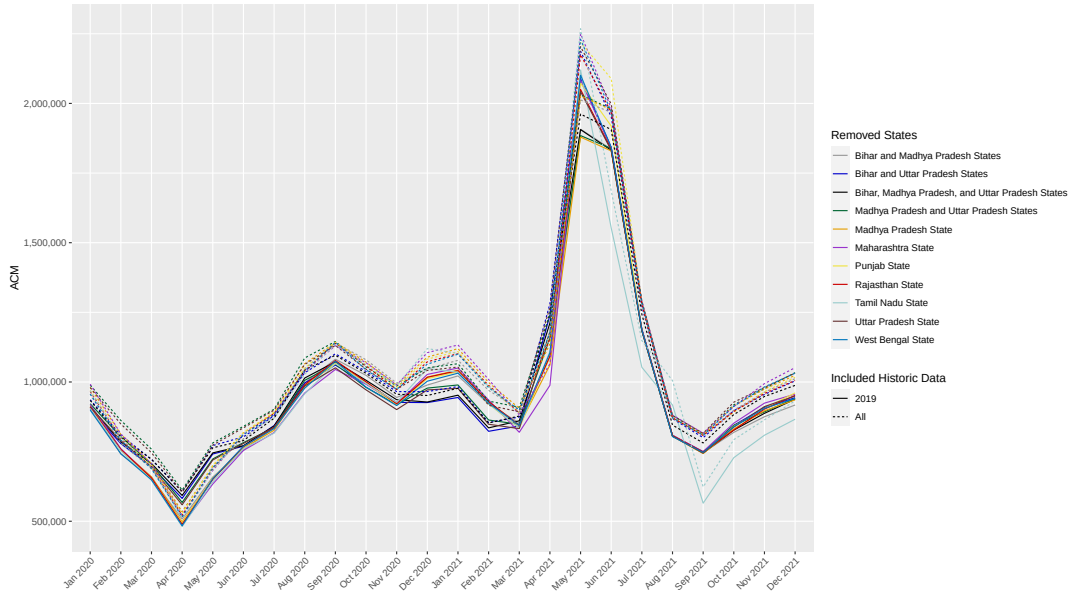

FIG 33. *Time series of ACM with different states excluded, and with different years of data used for the expected numbers.*

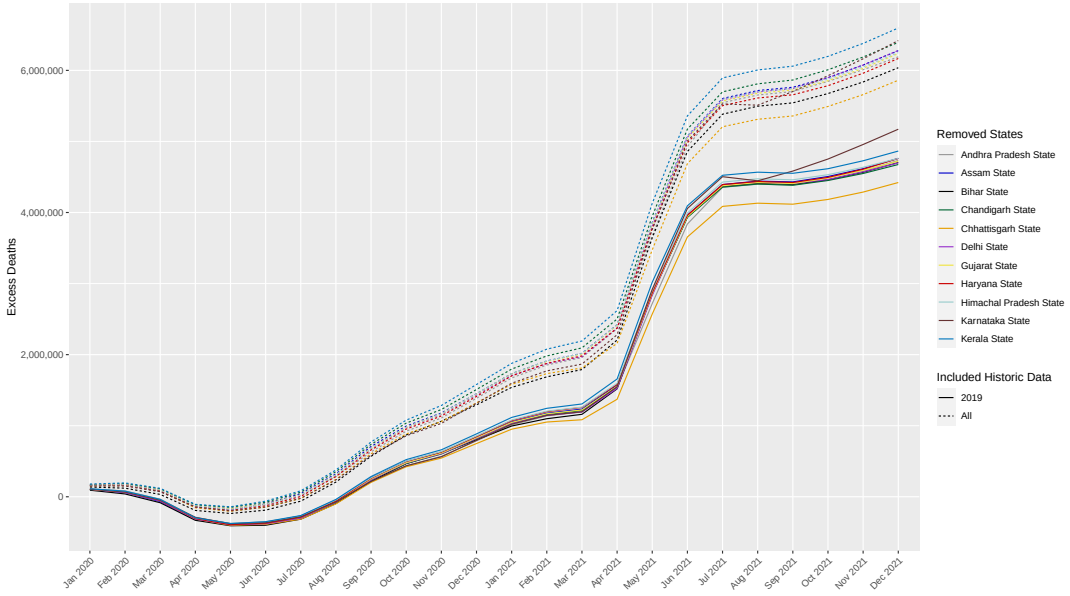

FIG 34. *Cumulative excess with different states excluded, and with different years of data used for the expected numbers. Based on all the data, we estimate that India's excess is 4.7 million deaths, with a 95% credible interval of (3.31, 6.48) million.*

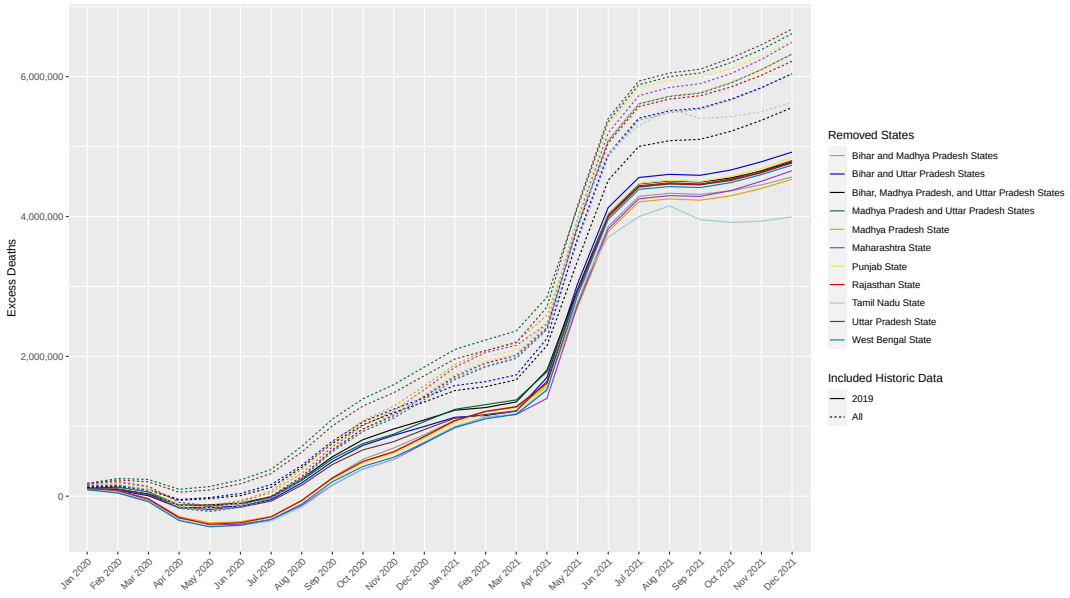

FIG 35. *Cumulative excess with different states excluded, and with different years of data used for the expected numbers. Based on all the data, we estimate that India's excess is 4.7 million deaths, with a 95% credible interval of (3.31, 6.48) million.*

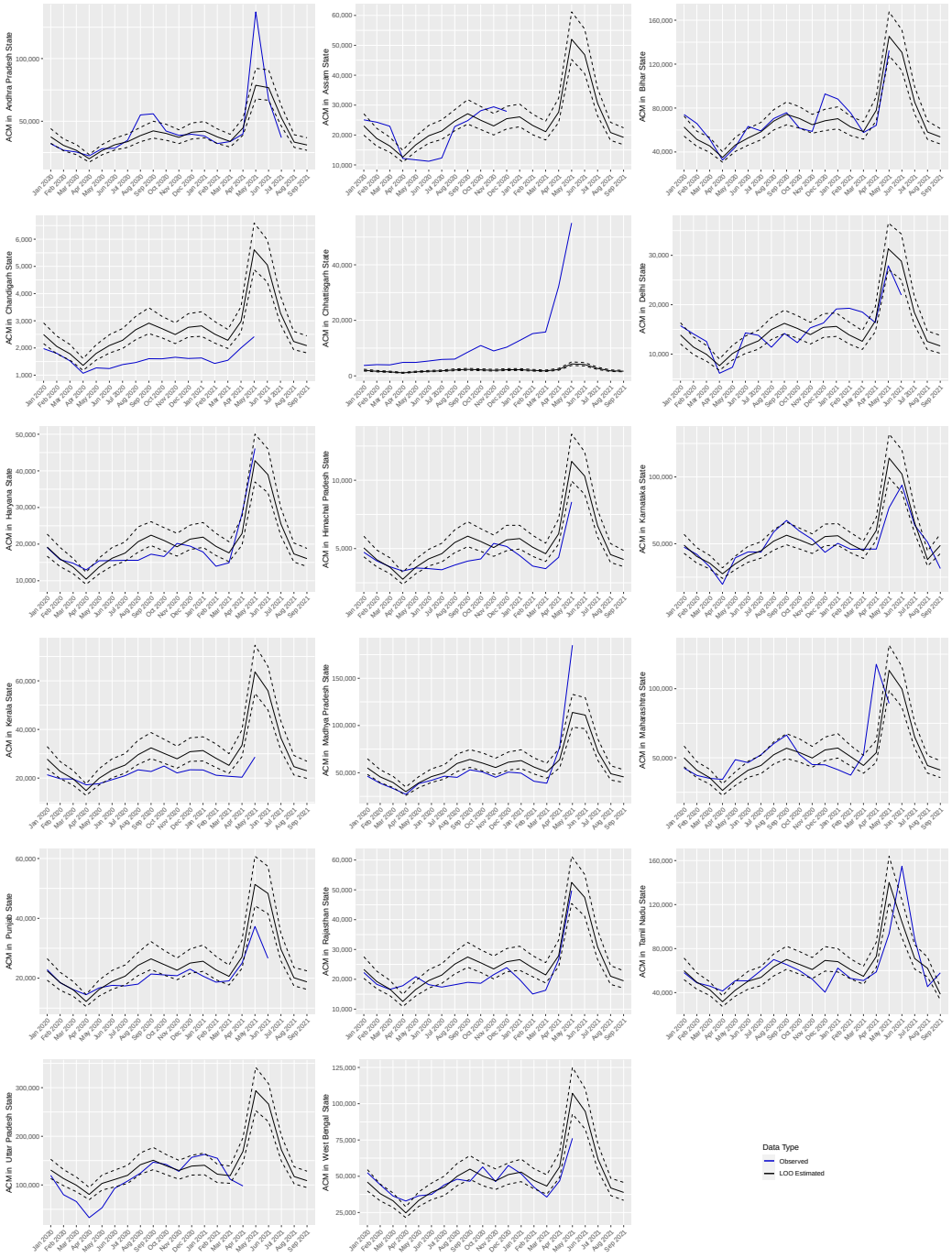

FIG 36. *Observed ACM by month and predicted, based on a leave-one-out procedure, in which the state ACM is predicted based on the data from all other states.*

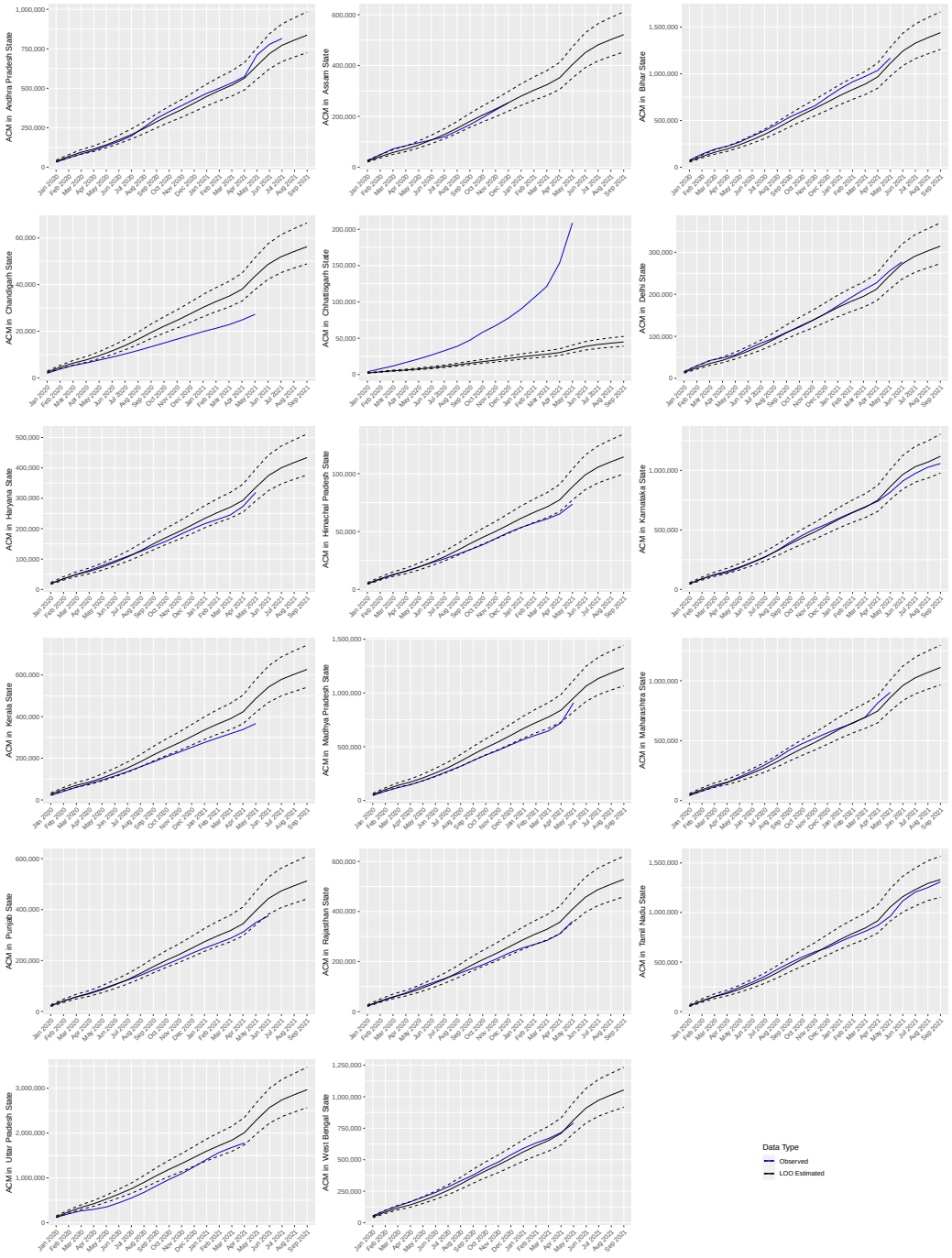

FIG 37. *Cumulative ACM by month and predicted, based on a leave-one-out procedure, in which the state ACM is predicted based on the data from all other states.*

In Table 3 we give our estimates (based on all data for the first 21 months and with expected numbers calculates from 2019) and also give the estimates from IHME, The Economist, Jha *et al.* (2022) and three estimates from Anand *et al.* (2021). The Jha *et al.* (2022) estimate is based on a nationally representative telephone survey, a government survey that covers 0.14 million adults and the Government of India's data from facility-based deaths and CRS deaths in 10 states. Anand *et al.* (2021) use three methods: Indian States' CRS (method 1), international age-specific infection fatality rates applied to Indian demography (method 2) and seroprevalence and a household survey (method 3).

There is reasonable agreement between the different estimates, which is reassuring, given the different data sources used. Along with the sensitivity and leave-one-out analyses, this provides further evidence that the model is reasonable and the subnational data (taken as a whole) are representative, so that, when combined, they provide a reliable excess mortality estimate.

Approach	**Estimate** $(\times 10^6)$	Period
Naive	5.04 (4.48, 5.59)	Jan 20–Dec 21
WHO	4.74 (3.31, 6.48)	Jan 20–Dec 21
The Economist	4.86 (1.70, 8.47)	Jan 20–Dec 21
IHME	4.07 (3.71, 4.36)	Jan 20–Dec 21
Naive	4.29 (4.00, 4.59)	June 20–June 21
WHO	4.33 (2.85, 6.13)	June 20–June 21
Jha *et al.* (2022)	3.23 (3.06, 3.39)	June 20–June 21
Naive	3.96 (3.62, 4.29)	April 20–June 21
WHO	3.99 (2.40, 5.95)	April 20–June 21
Anand *et al.* (2021) Method 1	3.4	April 20–June 21
Anand *et al.* (2021) Method 2	4.0	April 20–June 21
Anand *et al.* (2021) Method 3	4.9	April 20–June 21

TABLE 3

The parentheses give 95% uncertainty intervals. The Jha et al. *(2022) estimate is for excess COVID-19 deaths. The naive estimates are based on the ACM estimates $Y_{t,1}/\widehat{p}_t$ where $Y_{t,1}$ is the observed ACM from the available states, and $\widehat{p}_t$ is the estimated fraction of deaths available in month t.*

6.5. *Indonesia.* We have the annual number of national deaths in Indonesia as published by the Global Burden of Disease (GBD) Study from 2015–2019 GBD (2020). The subnational data consist of the monthly number of deaths from 2015–2021 from Jakarta, Indonesia. The proportions of deaths in Jakarta in 2015–2019 are shown in Figure 38. Note that this is only just above 3%. An alternative to using the Jakarta data, is to use the global covariate model. In Figure 39 we show the comparison between these two analyses (over the period January 2020–June 2021, in the last 6 months of 2021 there are no subnational data, and so the covariate model is used). For the covariate model the point and 95% interval estimate are 495K (256K, 726K) while for the subnational they are 1,024K (752K 1,287K). There are large differences in the two analyses, and in the main paper the subnational estimates were the ones we used when reporting regional and global estimates, as WHO liked to use observed data from a country, when available. We believe it is important to see both estimates, however, because of the small proportion of the population observed in an urban setting.

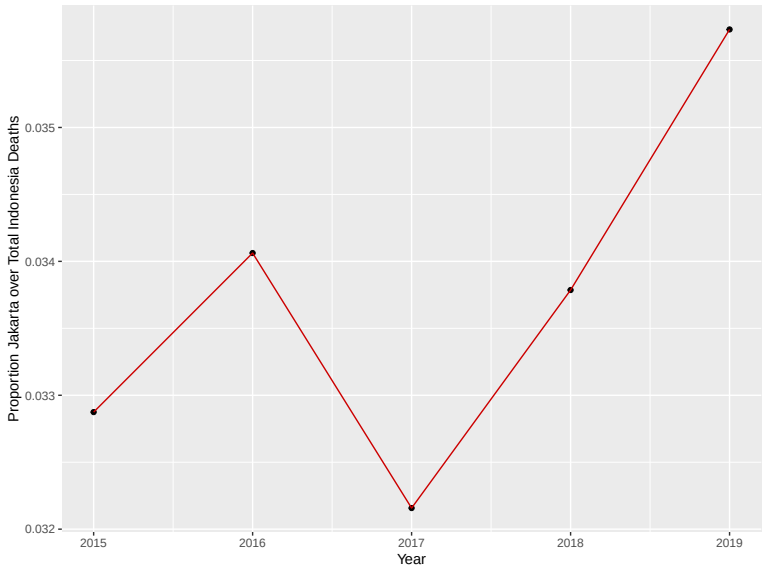

FIG 38. *Proportion of ACM counts in Jakarta in 2015–2019.*

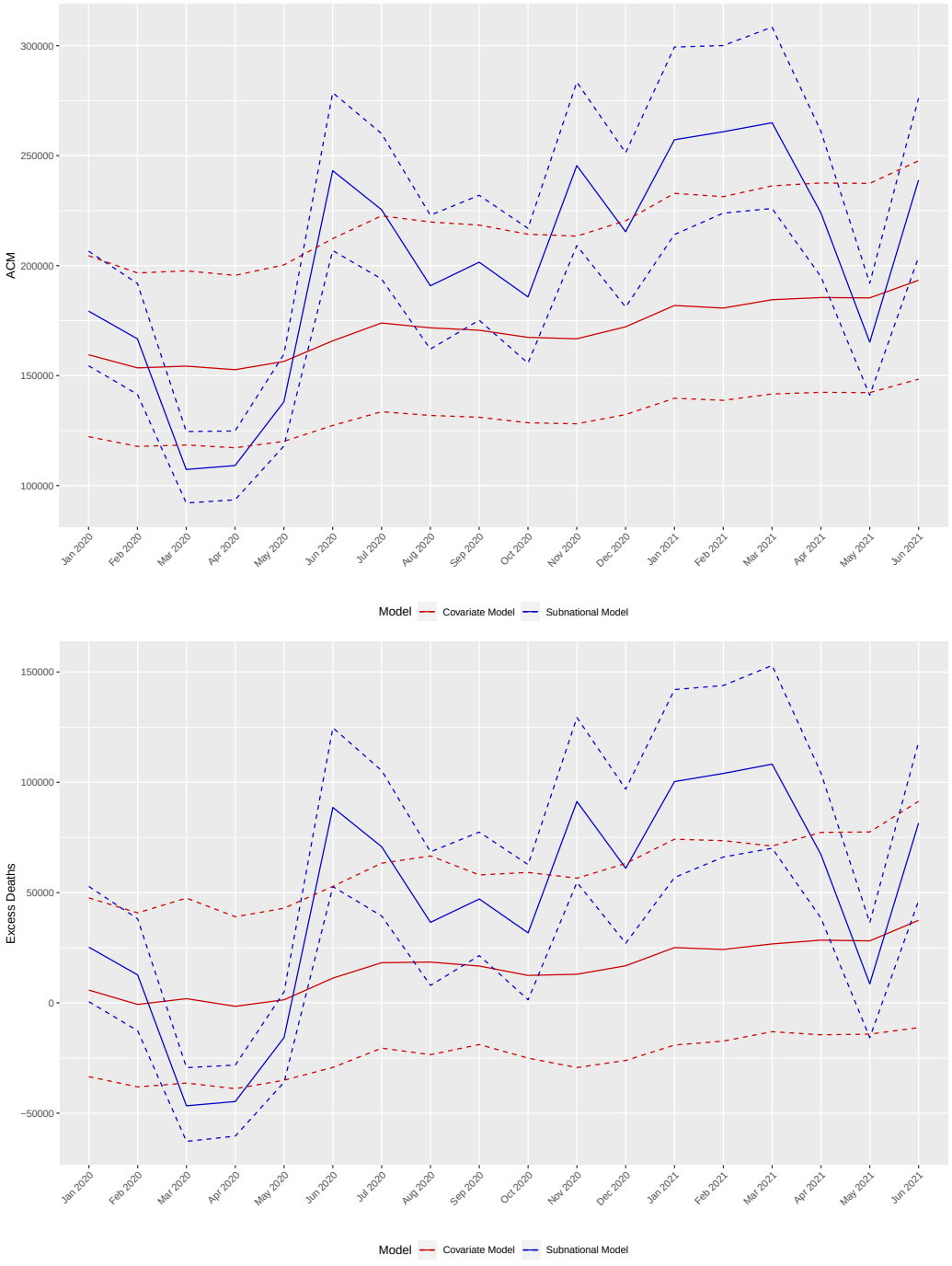

FIG 39. *Estimated ACM (top) and excess ACM (bottom) for Indonesia from covariate model and subnational data from Jakarta.*

6.6. *Turkey.* We have monthly annual deaths in Turkey as published by the Turkish National Statistics Office from 2015–2019. The subnational data correspond to monthly ACM counts from 2018–2021 in 24 provinces and cities from all over Turkey, as published by Guclu Yaman. More details, for 21 of the locations are at `https://gucluyaman.com/tr/excess-mortality-in-turkey/`.

Figure 40 shows the fractions of deaths in the 23 subnational areas over 2018–2019. Using the binomial subnational model, and the global covariate model, we obtain the estimates shown in Figure 41 – it is reassuring that they are so similar. In the main paper, we used the subnational estimates.

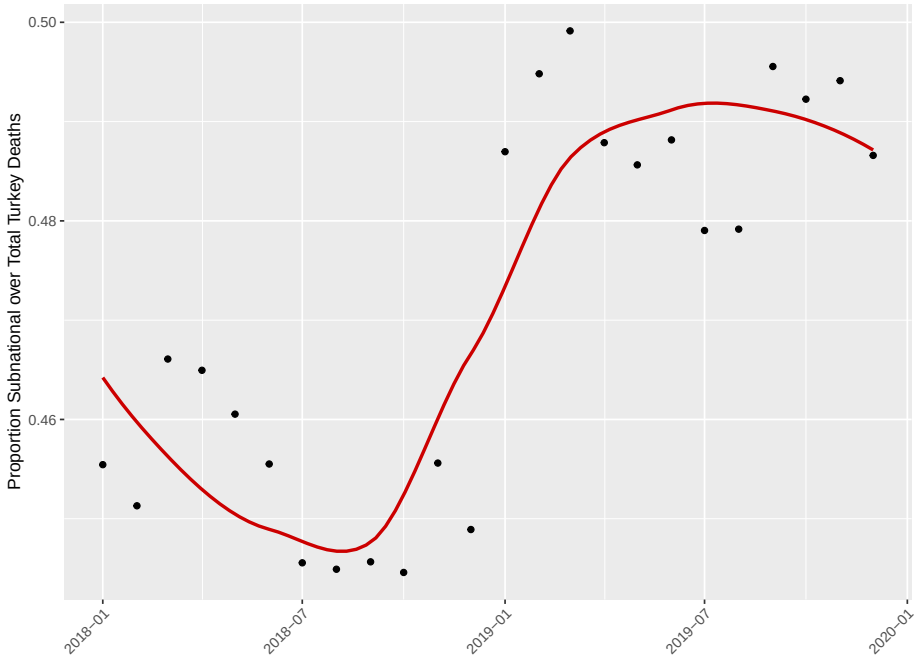

FIG 40. *Proportion of ACM counts in subregions of Turkey in 2015–2019.*

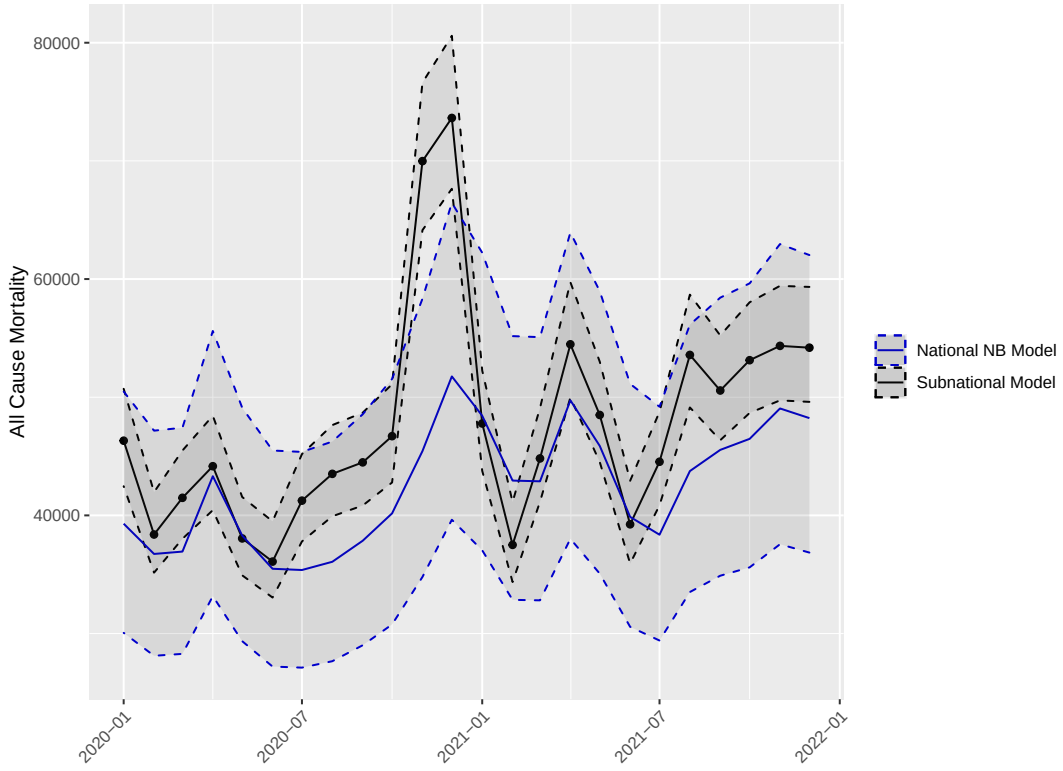

FIG 41. *Predicted ACM, with 95% uncertainty, for Turkey from covariate model and subnational model.*

6.7. *Additional Analyses for Germany and Sweden.* After the official release of the WHO results, there was attention on Germany and Sweden which has lead us to examine our models and data sources for those countries. The original excess estimate for Germany was 195K (161K, 229K). This estimate was obtained using a negative binomial model with a thin-plate spline for the annual trend (on the linear predictor scale). A scaling factor to account for completeness was also used, which lead the ACM counts in 2016–2018 to be scaled up. Unfortunately for the adjusted data the spline fit was unduly influenced by a lower count in 2019 which caused the spline prediction in the pandemic to be too low, and the excess correspondingly to be too high. We removed the completeness adjustment and replaced the spline term for the annual trend with a linear term, and this produced the much more reasonable series in the left-hand panel of Figure 42. This produces a revised excess estimate of 122K with a 95% interval of (101K, 143K). With the adjusted data, the spline also produced a reasonable fit (right-hand panel of Figure 42) and very similar estimates.

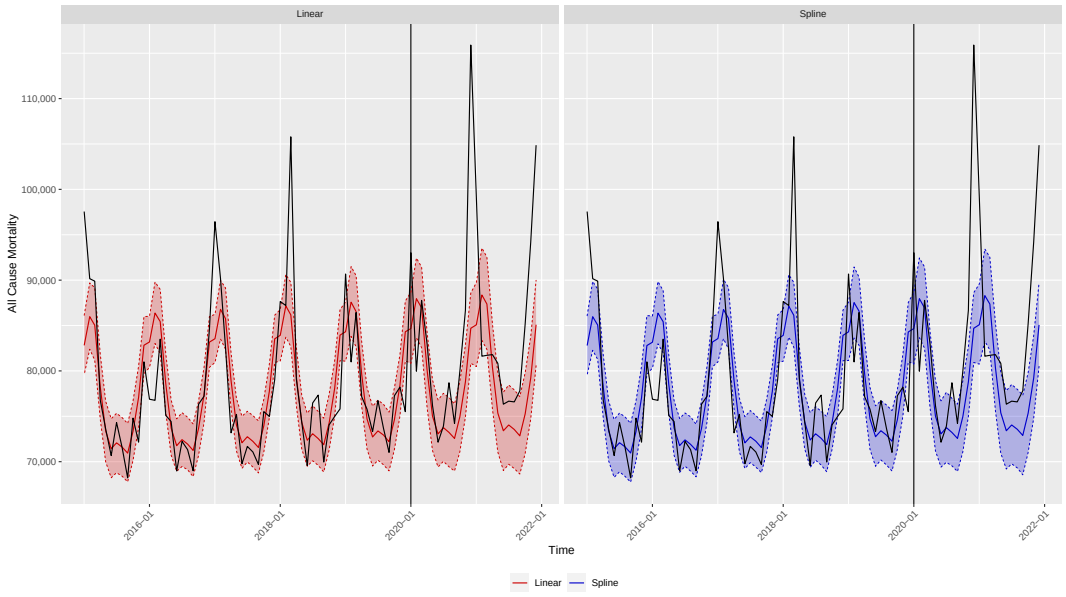

FIG 42. *Expected ACM counts and observed ACM (the black lines) for Germany, using unadjusted ACM data.*

For Sweden, the WHO made a completeness adjustment for the 2019 mortality count (which was lower than the previous year), which resulted in an increase in the count, and this same adjustment was also applied to the 2020 and 2021 counts. The original excess estimate for Sweden, using the adjusted data, was 11.3K (9.9K, 12.7K). With hindsight the adjustment was unnecessary and so we present here an analysis with the unadjusted data, and replacing the spline term for the annual trend with a linear term. The revised estimates with the unadjusted data are 13.4K (11.7K, 15.2K), so an increase over the previous analysis. With the unadjusted data the spline model gave similar excess estimates. The fits are shown in Figure 43. For the next update of estimates, we will revisit the completeness process that was used to produce the counts used in the various analyses, and also examine different models for calculating the expected numbers.

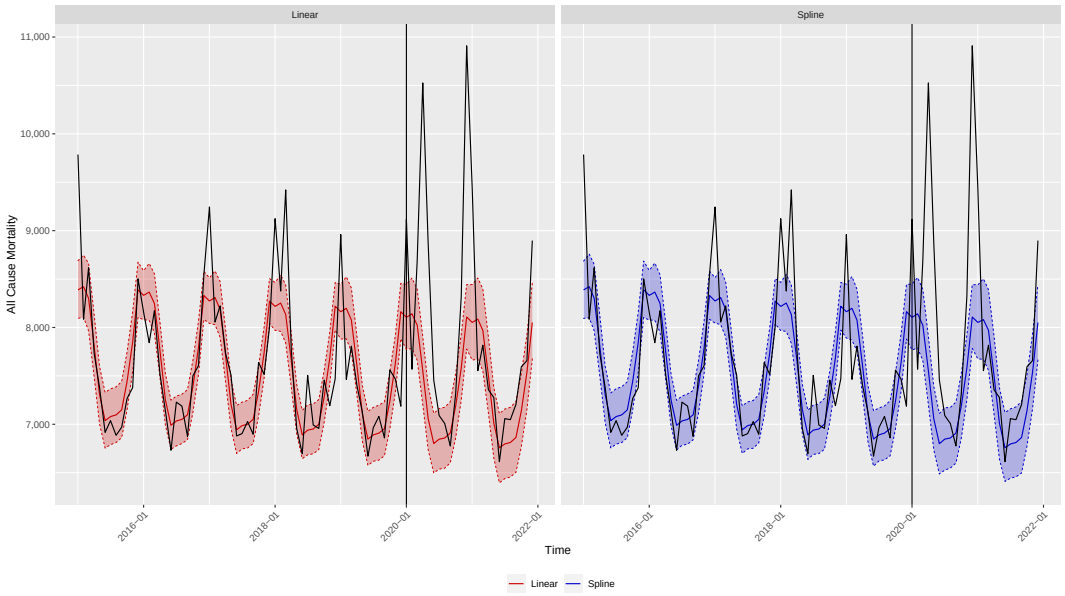

FIG 43. *Expected ACM counts and observed ACM (the black lines) for Sweden, using unadjusted ACM data.*

7. Supplementary Materials: Model Assessment. The sampling model we assume is,

$$Y_{c,t}|\theta_{c,t} \sim \text{NegBinl}(\widehat{E}_{c,t}\theta_{c,t}, \widehat{\tau}_{c,t})$$

with known overdispersion parameter $\widehat{\tau}_{c,t}$ and mean $\text{E}[Y_{c,t}|\theta_{c,t}] = \widehat{E}_{c,t}\theta_{c,t}$ and $\text{var}(Y_{c,t}|\theta_{c,t}) = \widehat{E}_{c,t}\theta_{c,t}\left(1 + \widehat{E}_{c,t}\theta_{c,t}/\widehat{\tau}_{c,t}\right)$ with

$$\log\theta_{c,t} = \alpha + \sum_{b=1}^{B}\beta_{bt}X_{bct} + \sum_{g=1}^{G}\gamma_g Z_{gc} + \epsilon_{c,t}, \tag{2}$$

and $\epsilon_{c,t} \sim_{iid} \text{N}(0, \sigma_\epsilon^2)$.

We wish to assess whether the covariate model provides a good fit to the data. To this end we perform a number of model checks.

7.1. *Fitted Values.* We plot fitted values $\widehat{y}_{c,t}$ versus observed values $y_{c,t}$. The fitted values are given by $\widehat{Y}_{c,t} = \widehat{E}_{c,t}\widehat{\theta}_{c,t}$ where $\widehat{\theta}_{c,t}$ is the posterior median. We color code the points by region. These plots are created both for in-sample in Figure 44, and out-of-sample (via cross-validation in which data from either a complete country or a complete month are removed) in Figure 45). As we would expect, the in-sample points almost all lie on the line of equality (since we include the random effects $\epsilon_{c,t}$ for each country-time point combination). The out-of-sample versions are less good, as expected, but nothing jumps out as being particularly aberrant.

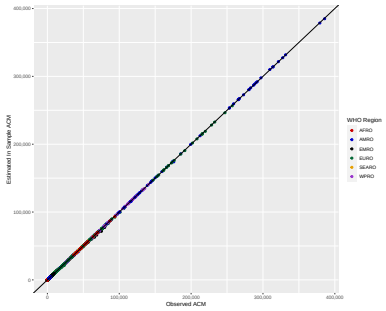

FIG 44. *In-sample observed versus predicted, color-coded by region.*

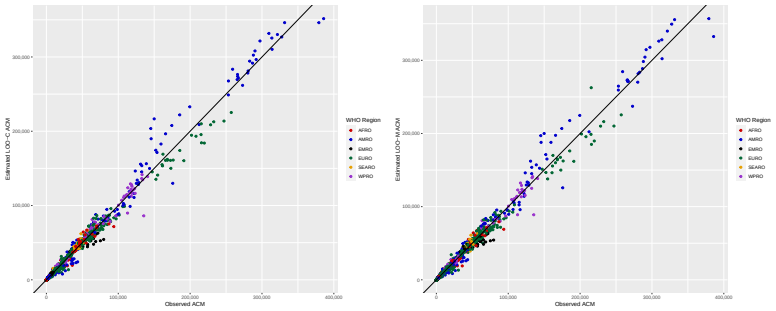

FIG 45. *Out-of-sample observed versus predicted: Left: country removed. Right: month removed. Color-coded by region.*

7.2. *Standardized Residuals.* We plot standardized residuals versus time (to see if there are is systematic model misspecification over time) and versus the log of the fitted values (to assess whether the mean-variance relationship is adequate), in both cases color coded by region. Standardized residuals are:

$$r_{c,t} = \frac{y_{c,t} - \widehat{y}_{c,t}}{\sqrt{\widehat{E}_{c,t}\widehat{\theta}_{c,t}\left(1 + \widehat{E}_{c,t}\widehat{\theta}_{c,t}/\widehat{\tau}_{c,t}\right)}}.$$

Figure 46 shows in-sample standardized residuals over time – it is difficult to make any definitive statements from this plot. There are some relatively high residuals for low fitted values, but the total number of such points is small, and their contribution to the overall excess picture is small (the countries with values below 5 in log fitted ACM are (in order from left to right in the plot) San Marino, Monaco, Saint Kitts and Nevis, Andorra, Antigua and Barbuda, Seychelles and the Maldives). Figure 47 shows absolute standardized residuals versus log fitted values, with a smoother added, for both in-sample and leave-one-out residuals. In both plots, there is no systematic pattern for larger values, which is important, as this would indicate a deficiency in the mean-variance relationship.

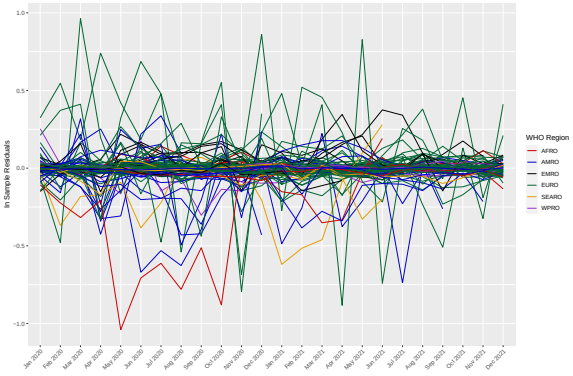

FIG 46. *In-Sample standardized residuals over time, color-coded by region.*

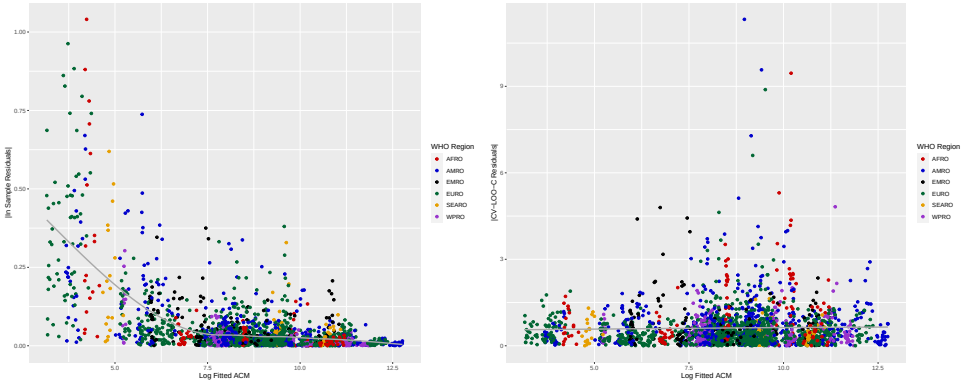

FIG 47. *Absolute values of residuals versus log fitted values. Left: In-sample versions. Right: Leave-one-country out versions. Smoothers are drawn on each.*

7.3. *Bias and RMSE.* We assess the errors in our model, also using CV, over the countries with ACM data. Let $r_{c,t} = Y_{c,t}/N_{c,t}$ be the observed ACM rate and $\widehat{r}_{c,t} = \widehat{Y}_{c,t}/N_{c,t}$ where $\widehat{Y}_{c,t} = \text{PostMedian}(Y_{c,t}|\boldsymbol{y}_{-ct})$ is the estimated rate. We report the relative bias of the ACM rate,

$$\frac{1}{\sum_c |M_c|} \sum_c \sum_{t \in M_c} \frac{\widehat{r}_{c,t} - r_{c,t}}{r_{c,t}}, \tag{3}$$

and the absolute version of this quantity,

$$\frac{1}{\sum_c |M_c|} \sum_c \sum_{t \in M_c} \frac{|\widehat{r}_{c,t} - r_{c,t}|}{r_{c,t}}. \tag{4}$$

These measures can be calculated with the estimated rates being based on data with either a complete country's worth of data or a complete months worth of data being left out.

We also calculate the root mean squared error (RMSE) of the fit:

$$\sqrt{\frac{1}{\sum_c |M_c|} \sum_c \sum_{t \in M_c} (\widehat{r}_{c,t} - r_{c,t})^2}$$

again using the two cross-validation schemes (by month and by country). We also estimate the coverage of the predictive intervals from these CV exercises, at the 50%, 80% and 95% levels.

Table 4 shows the summaries. The relative biases are small (just under 2%), while the absolute relative biases are around 10%. The RMSE measures are around 1.25×10^3. Under both CV schemes, the coverages are a little higher than the nominal for the 50% and 80% levels and a little lower than the nominal for the 95% level.

CV Level	Measure	Performance
Country	Relative Bias	1.98
Country	Absolute Relative Bias	10.08
Country	RMSE ($\times$1000)	1.25
Country	Coverage: 50% Interval	59.3
Country	Coverage: 80% Interval	82.7
Country	Coverage: 95% Interval	91.6
Month	Relative Bias	1.84
Month	Absolute Relative Bias	10.18
Month	RMSE ($\times$1000)	1.24
Month	Coverage: 50% Interval	57.8
Month	Coverage: 80% Interval	83.7
Month	Coverage: 95% Interval	92.9

TABLE 4

Leave one country and month out model assessment measures. Relative bias and absolute relative bias are expressed as percentages.

8. Supplementary Materials: Data Types By Country. On the following pages we list the countries for which we produced excess mortality estimates, along with the regions within which they lie, and the type of data they have available.

Country List		
Country	WHO Region	Data Type
Afghanistan	EMRO	No Data
Albania	EURO	Full National
Algeria	AFRO	Partial National
Andorra	EURO	Partial National
Angola	AFRO	No Data
Antigua and Barbuda	AMRO	Partial National
Argentina	AMRO	Partial National / Sub-national Data
Armenia	EURO	Full National
Australia	WPRO	Full National
Austria	EURO	Full National
Azerbaijan	EURO	Full National
Bahamas	AMRO	No Data
Bahrain	EMRO	No Data
Bangladesh	SEARO	No Data
Barbados	AMRO	Partial National
Belarus	EURO	Partial National
Belgium	EURO	Full National
Belize	AMRO	Partial National
Benin	AFRO	No Data
Bhutan	SEARO	No Data
Bolivia (Plurinational State of)	AMRO	Full National
Bosnia and Herzegovina	EURO	Full National
Botswana	AFRO	No Data
Brazil	AMRO	Full National
Brunei Darusssalam	WPRO	Partial National
Bulgaria	EURO	Full National
Burkina Faso	AFRO	No Data
Burundi	AFRO	No Data
Cabo Verde	AFRO	No Data
Cambodia	WPRO	No Data
Cameroon	WPRO	No Data
Canada	AMRO	Partial National
Central African Republic	AFRO	No Data
Chad	AFRO	No Data
Chile	AMRO	Full National
China	WPRO	Annual Data
Colombia	AMRO	Full National
Comoros	AFRO	No Data
Congo	AFRO	No Data
Cook Islands	WPRO	No Data
Costa Rica	AMRO	Partial National
Côte d'Ivoire	AFRO	No Data
Croatia	EURO	Full National
Cuba	AMRO	Partial National
Cyprus	EURO	Full National
Czechia	EURO	Full National
Democratic People's Republic of Korea	SEARO	No Data
Democratic Republic of the Congo	AFRO	No Data
Denmark	EURO	Full National

Country List		
Country	WHO Region	Data Type
Djibouti	EMRO	No Data
Dominica	AMRO	No Data
Dominican Republic	AMRO	Partial National
Ecuador	AMRO	Full National
Egypt	EMRO	Partial National
El Salvador	AMRO	Partial National
Equatorial Guinea	AFRO	No Data
Eritrea	AFRO	No Data
Estonia	EURO	Full National
Eswatini	AFRO	No Data
Ethiopia	AFRO	No Data
Fiji	WPRO	No Data
Finland	EURO	Full National
France	EURO	Full National
Gabon	AFRO	No Data
Gambia	AFRO	No Data
Georgia	EURO	Partial National
Germany	EURO	Full National
Ghana	AFRO	No Data
Greece	EURO	Full National
Grenada	AMRO	Annual Data
Guatemala	AMRO	Full National
Guinea	AFRO	No Data
Guinea-Bisssau	AFRO	No Data
Guyana	AMRO	No Data
Haiti	AMRO	No Data
Honduras	AMRO	No Data
Hungary	EURO	Full National
Iceland	EURO	Full National
India	SEARO	Subnational Data
Indonesia	SEARO	Subnational Data
Iran (Islamic Republic of)	EMRO	Full National
Iraq	EMRO	Partial National
Ireland	EURO	Full National
Israel	EURO	Full National
Italy	EURO	Full National
Jamaica	AMRO	Partial National
Japan	WPRO	Full National
Jordan	EMRO	Partial National
Kazakhstan	EURO	Full National
Kenya	AFRO	Full National
Kiribati	WPRO	No Data
Kuwait	EMRO	Partial National
Kyrgyzstan	EURO	Full National
Lao People's Democratic Republic	WPRO	No Data
Latvia	EURO	Full National
Lebanon	EMRO	Full National
Lesotho	AFRO	No Data
Liberia	AFRO	No Data
Libya	EMRO	No Data
Lithuania	EURO	Full National
Luxembourg	EURO	Full National
Madagascar	AFRO	No Data

Country List		
Country	WHO Region	Data Type
Malawi	AFRO	No Data
Malaysia	WPRO	Partial National
Maldives	SEARO	Partial National
Mali	AFRO	No Data
Malta	EURRO	Full National
Marshall Islands	WPRO	No Data
Mauritania	AFRO	No Data
Mauritius	AFRO	Full National
Mexico	AMRO	Full National
Micronesia (Federated States of)	WPRO	No Data
Monaco	EURO	Full National
Mongolia	WPRO	Full National
Montenegro	EURO	Partial National
Morocco	EMRO	No Data
Mozambique	AFRO	No Data
Myanmar	SEARO	No Data
Namibia	AFRO	No Data
Nauru	WPRO	No Data
Nepal	SEARO	No Data
Netherlands	EURO	Full National
New Zealand	WPRO	Full National
Nicaragua	AMRO	Partial National
Niger	AFRO	No Data
Nigeria	AFRO	No Data
Niue	WPRO	No Data
North Macedonia	EURO	Full National
Norway	EURO	Full National
Oman	EMRO	Full National
Pakistan	EMRO	No Data
Palau	WPRO	No Data
Panama	AMRO	Partial National
Papua New Guinea	WPRO	No Data
Paraguay	AMRO	Full National
Peru	AMRO	Full National
Phillipines	WPRO	Partial National
Poland	EURO	Full National
Portugal	EURO	Full National
Qatar	EMRO	Full National
Republic of Korea	WPRO	Full National
Republic of Moldova	EURO	Full National
Romania	EURO	Full National
Russian Federation	EURO	Full National
Rwanda	AFRO	No Data
Saint Kitts and Nevis	AMRO	Annual Data
Saint Lucia	AMRO	No Data
Saint Vincent and the Grenadines	AMRO	Annual Data
Samoa	WPRO	No Data
San Marino	EURO	Full National
Sao Tome and Principe	AFRO	No Data
Saudi Arabia	EMRO	No Data
Senegal	AFRO	No Data

Country List		
Country	WHO Region	Data Type
Serbia	EURO	Full National
Seychelles	AFRO	Partial National
Sierra Leone	AFRO	No Data
Singapore	WPRO	Full National
Slovakia	EURO	Full National
Slovenia	EURO	Full National
Solomon Islands	WPRO	No Data
Somalia	EMRO	No Data
South Africa	AFRO	Full National
South Sudan	AFRO	No Data
Spain	EURO	Full National
Sri Lanka	SEARO	Annual Data
Sudan	EMRO	No Data
Suriname	AMRO	Partial National
Sweden	EURO	Full National
Switzerland	EURO	Full National
Syrian Arab Republic	EMRO	No Data
Tajikistan	EURO	Partial National
Thailand	SEARO	Full National
The United Kingdom	EURO	Full National
Timor-Leste	SEARO	No Data
Togo	AFRO	Full National
Tonga	WPRO	No Data
Trinidad and Tobago	AMRO	No Data
Tunisia	EMRO	Partial National
Turkey	EURO	Subnational Data
Turkmenistan	EURO	No Data
Tuvalu	WPRO	No Data
Uganda	AFRO	No Data
Ukraine	EURO	Full National
United Arab Emirates	EMRO	No Data
United Republic of Tanzania	AFRO	No Data
United States of America	AMRO	Full National
Uruguay	EURO	Full National
Uzbekistan	EURO	Full National
Vanuatu	WPRO	No Data
Venezuela (Bolivarian Republic of)	AMRO	No Data
Viet Nam	WPRO	Annual Data
Yemen	EMRO	No Data
Zambia	AFRO	No Data
Zimbabwe	AFRO	No Data

TABLE 5
Countries, regions and data scenarios

REFERENCES

Anand, A., Sandefur, J., Subramanian, A., *et al.* (2021). *Three new estimates of India's all-cause excess mortality during the COVID-19 pandemic*. Center for Global Development.

Baker, S. G. (1994). The multinomial-Poisson transformation. *Journal of the Royal Statistical Society: Series D*, **43**, 495–504.

Besson, E. S. K., Norris, A., Ghouth, A. S. B., Freemantle, T., Alhaffar, M., Vazquez, Y., Reeve, C., Curran, P. J., and Checchi, F. (2021). Excess mortality during the COVID-19 pandemic: a geospatial and statistical analysis in Aden governorate, Yemen. *BMJ Global Health*, **6**, e004564.

DeGennaro, V., Schwartz, T., Henderson, R., and Elie, M.-C. (2021). A cross-sectional cohort study of prevalence of antibodies to COVID-19 in Port-au-Prince, Haiti. *medRxiv*.

EFE (2021). Honduras acumula 9.679 muertes por covid-19 tras 18 meses del primer deceso.

GBD (2020). Global burden of 369 diseases and injuries in 204 countries and territories, 1990–2019: a systematic analysis for the Global Burden of Disease Study 2019. *The Lancet*, **396**, 1204–1222.

Hamukale, A., Hines, J. Z., Sinyange, N., Fwoloshi, S., Malambo, W., Sivile, S., Chanda, S., Mucheleng'anga, L. A., Kayeyi, N., Himwaze, C. M., Shibemba, A., Leigh, T., Mazaba, M. L., Kapata, N., Zulu, P., Zyambo, K., Mupeta, F., Agolory, S., Mulenga, L. B., Malama, K., and Kapina, M. (2021). SARS-CoV-2 mortality surveillance among community deaths brought to university teaching hospital mortuary in Lusaka, Zambia, 2020. *medRxiv*.

Hanifi, S. M. A., Alam, S. S., Shuma, S. S., and Reidpath, D. D. (2021). Insights into excess mortality during the first months of the COVID-19 pandemic from a rural, demographic surveillance site in Bangladesh. *Frontiers in Public Health*, **9**, 1016.

Jha, P., Deshmukh, Y., Tumbe, C., Suraweera, W., Bhowmick, A., Sharma, S., Novosad, P., Fu, S. H., Newcombe, L., Gelband, H., *et al.* (2022). COVID mortality in India: National survey data and health facility deaths. *Science*, page eabm5154.

Jorari, L. (2021). Mass burial to relieve overflowing Papua New Guinea morgue as Covid cases surge. *The Guardian*.

Karlinsky, A. and Kobak, D. (2021). Tracking excess mortality across countries during the COVID-19 pandemic with the World Mortality Dataset. *eLife*, **10**, e69336.

Kirmani, S., Zahid, U., and Hussain, A. (2020). In the days of the epidemic, the number of deaths in Karachi and Lahore in the month of June increased significantly as compared to 2019.

Moser, W., Fahal, M. A. H., Abualas, E., Bedri, S., Elsir, M. T., Mohamed, M. F. E. R. O., Mahmoud, A. B., Ahmad, A. I. I., Adam, M. A., Altalib, S., DafaAllah, O. A., Hmed, S. A., Azman, A. S., Ciglenecki, I., Gignoux, E., González, A., Mwongera, C., and Albela, M. (2021). Retrospective mortality and prevalence of SARS-CoV-2 antibodies in greater Omdurman, Sudan: a population–based cross–sectional survey. *medRxiv*.

Mwananyanda, L., Gill, C. J., MacLeod, W., Kwenda, G., Pieciak, R., Mupila, Z., Lapidot, R., Mupeta, F., Forman, L., Ziko, L., Etter, L., and Thea, D. (2021). Covid-19 deaths in Africa: prospective systematic postmortem surveillance study. *BMJ*, **372**.

National Bureau of Statistics of China (2021). China statistical yearbook.

National Bureau of Statistics of China (2022). Press release january 17th 2022.

NDTV.com (2022). Bihar Saw Nearly 75,000 Unaccounted Deaths Amid 2nd Covid Wave, Data Shows.

News, B. (2020). "Thousands of stories of grief": An investigation reveals death numbers and frightening statistics.

Office Of The Registrar General (2021). Vital statistics of India based on the civil registration system 2019.

Parkinson, J. (2021). Inside the world's most blatant Covid-19 coverup: Secret burials, a dead president. *Wall Street Journal*.

Qi, J., Zhang, D., Zhang, X., Takana, T., Pan, Y., Yin, P., Liu, J., Liu, S., Gao, G. F., He, G., and Zhou, M. (2022). Short- and medium-term impacts of strict anti-contagion policies on non-COVID-19 mortality in China. *Nature Human Behaviour*, **6**, 55–63.

Rahman, A., Hossain, A., Ameen, S., Ahmed, A., Mhajabin, S., Haider, M., Rahman, H., Nusrat, N., Sania, A., Chowdhury, A., and Arifeen, S. (2021a). Pr-20107: Estimating the excess mortality during covid-19 pandemic and strengthening the record keeping system of the burial sites. *Mimeo*.

Rahman, A., Hossain, A., Ameen, S., Ahmed, A., Siddique, A., Mhajabin, S., Haider, M., Akter, E., Sania, A., Chowdhury, A., and SE, A. (2021b). Pr-20108: Estimating the impact of covid-19 pandemic on mortality rates among older adult population in selected geography in chattogram (chittagong). *Mimeo*.

Ramani, S. (2021a). 'Excess deaths' in Haryana seven times official COVID-19 toll. *The Hindu*.

Ramani, S. (2021b). 'Excess deaths' in Kerala 1.6 times official COVID-19 toll. *The Hindu*.

Ramani, S. (2021c). Excess deaths in Maharashtra were at least 3 times the official COVID toll. *The Hindu*.

Ramani, S. (2021d). Excess deaths in Rajasthan are at least five times the official COVID-19 tally. *The Hindu*.

Ramani, S. (2021e). Excess deaths in West Bengal 11 times official COVID-19 tally. *The Hindu*.

Ramani, S. (2021f). Himachal Pradesh 'excess deaths' twice the official COVID-19 toll. *The Hindu*.

Ramani, S. and Radhakrishnan, V. (2021). Chhattisgarh's excess deaths at least 4.8 times COVID-19 toll. *The Hindu*.

Ramani, S. and Vasudeva, V. (2021a). Coronavirus | Chandigarh bucks 'excess deaths' trend. *The Hindu*.

Ramani, S. and Vasudeva, V. (2021b). Coronavirus | Punjab 'excess deaths' three times official toll. *The Hindu*.

Rao, C. and Gupta, M. (2020). The civil registration system is a potentially viable data source for reliable subnational mortality measurement in india. *BMJ global health*, **5**(8), e002586.

Rukmini, S. (2022a). Andhra Pradesh saw 400% increase in deaths in May, Tamil Nadu saw more modest excess mortality. *Scroll.in*.

Rukmini, S. (2022b). Madhya Pradesh saw nearly three times more deaths than normal after second wave of Covid-19 struck. *Scroll.in*.

Saikia, A. (2022). Assam saw 28,000 more deaths than normal in months when first wave of Covid-19 struck. *Scroll.in*.

Staff, S. (2022). UP: 24 districts reported 110% more deaths between July and March than same period the previous year. *Scroll.in*.

The Times of India (2021). Covid second wave: 19,000 death certificates in Delhi nearly double of June 2020.

Wakefield, J., Haneuse, S., Dobra, A., and Teeple, E. (2011). Bayes computation for ecological inference. *Statistics in Medicine*, **30**, 1381–1396.

Watson, O. J., Alhaffar, M., Mehchy, Z., Whittaker, C., Akil, Z., Brazeau, N. F., Cuomo-Dannenburg, G., Hamlet, A., Thompson, H. A., Baguelin, M., *et al.* (2021). Leveraging community mortality indicators to infer COVID-19 mortality and transmission dynamics in Damascus, Syria. *Nature Communications*, **12**(1), 1–10.

WHO (2020). WHO methods and data sources for life tables 1990–2019. Technical report, Department of Data and Analytics, Division of Data, Analytics and Delivery for Impact, WHO, Geneva.

Wood, S. N. (2017). *Generalized Additive Models: An Introduction with R, Second Edition*. CRC Press.

Zeng, X., Adair, T., Wang, L., Yin, P., Qi, J., Liu, Y., Liu, J., Lopez, A. D., and Zhou, M. (2020). Measuring the completeness of death registration in 2844 Chinese counties in 2018. *BMC Medicine*, **18**(1), 176.